이학석사학위논문

Ruthenium Olefin Metathesis Catalysts Bearing Chelating *N*-Vinyl Lactam Ligands: Synthesis, Structure, and Reactivity

N-비닐 락탐 배위 루테늄 올레핀 메타테시스 촉매의 합성, 구조 및 반응성 연구

2015 년 8 월

서울대학교 대학원

화학부 유기화학 전공

김 민 하

Abstract

Ruthenium Olefin Metathesis Catalysts Bearing Chelating *N*-Vinyl Lactam Ligands: Synthesis, Structure, and Reactivity

Min Ha Kim
Department of Chemistry
The Graduate School
Seoul National University

Novel, phosphine-free ruthenium carbene complexes with carbonyl-chelating lactam ligand were synthesized. X-ray crystallography confirmed intramolecular coordination of pendant carbonyl group. Highly electron donating nature of Fischer carbenes induced great stability to the compounds. The complexes could catalyze olefin metathesis and cycloisomerization reaction depending on solvent and temperature conditions. Additionally, their structural peculiarity of *cis*- and *trans*-dichloro geometry was studied by NMR analysis.

Keywords **:** Olefin metathesis, ruthenium, organometallics, catalysis, cycloisomerization, carbene

Student Number : 2013-22917

Table of Contents

List of Figures

List of Schemes

List of Charts

List of Tables

Introduction

In recent decades, olefin metathesis emerged as a versatile tool for organic synthesis and polymer chemistry.[1-3] It is a unique carbon-carbon bond formation reaction which redistributes the fragments of alkenes across the double bond to furnish partner-changed olefins via metallacyclobutane intermediate. The evolution of this methodology was accelerated after the development of well-defined Ru, Mo, and W catalysts and study of mechanism.[4,5] Among a variety of the catalysts, ruthenium carbene complexes are especially advantageous because they are less sensitive toward air and moisture with their high reactivity and selectivity remained.[6] Development of modern ruthenium olefin metathesis catalysts has been aimed at increasing their selectivity as well as reactivity by modification of structure.

The first breakthrough in catalyst development was achieved by replacement of one phosphine ligand by *N*-heterocyclic carbene (NHC), which led to the second generation ruthenium olefin metathesis catalyst (complex 1, Figure 1).[7] This complex exhibits distinctly higher reactivity and functional group tolerance compared to its parental bisphosphine first generation complex. Soon after, chelation of styrenyl ether resulted Hoveyda-type complexes, of which their stability were highly improved (complex 2, Figure 1).[8] As the Hoveyda-type complexes proved, additional chelation to the metal center contributes to thermal, air, and moisture stability. Although

various chelated ruthenium alkylidene complexes were reported to be sufficiently reactive, most of the chelating ligands suffer from tedious synthetic problems. Such drawbacks also hindered the systematic study of electronic variation of the ligands, which is valuable for development of more efficient catalysts.[9,10] While the stability is increased adopting chelation of styrenyl ether moiety, fast initiation was achieved by replacing the phosphine ligand with more labile ligands (complex 3, Figure 1). Fast initiation is crucial for polymer synthesis since the initial reaction rate affects the important characters of the polymeric product, for example, average molecular weight or polydispersity index.

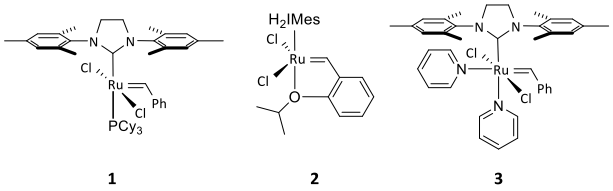

Figure 1. Commonly used Ru olefin metathesis catalysts

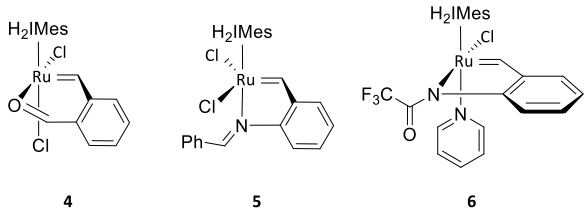

Figure 2. Selected examples of *N*- and *O*-chelated Ru olefin metathesis catalysts[11-14]

Chelated Ru carbene complexes with various electron-donating ligands were reported, and the representative examples are shown in Figure 2. In most cases, supplementary coordination resulted stabilization, or even latency to the catalysts.

Most of the well-defined ruthenium olefin metathesis catalysts have a square-pyramidal coordination of Ru center with *trans*-halido geometry.[15] In 1999, Hoffmann et al. reported one exceptional example, which was triggered by chelating bisphosphine ligand. In such complexes, P-Ru-Cl *trans* (i.e. Cl-Ru-Cl *cis*) arrangement was forced. Since the dissociation of the neutral ligand is required for the initiation of the catalytic cycle, appropriate design of this leaving ligand can accelerate or retard the initiation rate. Control of the initiation rate is of high interest for chemists since it often provides a clue for the entire reaction time. Especially in polymer chemistry, polymer with even distribution of molecular weight can only be obtained under the initiation in an instant. This is usually achieved by utilizing so-called latent catalysts, which are activated by external stimuli such as thermal, photo, or chemical treatment.[16]

Amide bonds are ubiquitous in both nature and chemical industry, for example, it is a key structural unit in peptides and one of the most pervasive source for polymers. Since amides contain carbonyl group which can coordinate to the metal center, they can be considered as a suitable candidate as a chelating ligand. The comprehensive study of complexes with electron-rich carbenes such as ethyl vinyl ether, vinyl sulfide, *N*-vinyl carbazole, and *N*-vinyl pyrrolidinone was conducted by Grubbs and co-worker.[17] Whilst such Fischer-type Ru complexes

had been reported to be relatively inert toward olefin metathesis reactions,[18] comparable reactivity was observed for some series of the complexes. Interestingly, it was reported that intramolecular coordination of the amide carbonyl group was detected in the ^{1}H NMR spectrum.[17,19]

Inspired by the combination of strongly electron donating character of Fischer carbene and carbonyl chelation which could result balance in stability and reactivity, we aimed at synthesis of ruthenium olefin metathesis catalysts with chelating *N*-vinyl lactam ligands. Herein, we report the synthesis, characterization, and reactivity of the complexes.

Results and Discussion

Catalyst Synthesis. The catalysts were synthesized from readily available *N*-vinyl lactams. The first attempts to synthesize lactam-chelated complex via reaction of phosphine-containing complex (1) didn't afford the products clearly. From the in situ NMR study of the reaction between complex 1 and vinyl lactam, we could observe that phosphine remained in the mixture. Although 1.1 to 1.5 equivalence of copper (I) chloride was added to thoroughly remove phosphine residue, chelated phosphine-free complex was not affordable. Inspired by lability of pyridine ligand, problematic phosphine ligand was replaced with pyridine. Finally, successful synthesis of lactam-chelated complexes as pale grey solid was achieved (Scheme 1). Products were purified by recrystallization in diethyl ether and yields were 60% (7a) or 40% (7b). Attempts to increase the yield by driving the equilibrium using large equivalence of lactam (up to 5 equiv.) resulted slightly negative effect due to excess amount of diethyl ether used during washing.

Scheme 1. Synthesis of catalysts with *N*-vinyl amides

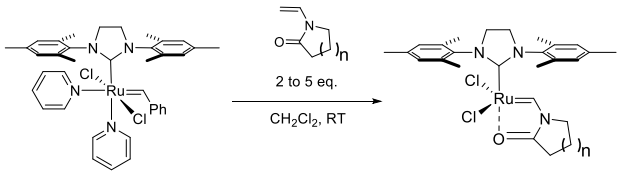

3 **7**
(**7a**: n=1, **7b**: n=3)

Characterization and Structural Peculiarity. Substitution reaction of complex **3** using commercially available *N*-vinylcaprolactam was performed (Scheme 1) to afford complex **7b.** To monitor the formation progress of chelated Fischer carbene complex, ^{1}H NMR was employed using characteristic chemical shift of the carbonic proton, from which 19.0 ppm from **3** was completely disappeared concomitant appearance of 13.4 ppm in the formation of complex **7b** after 3 hours. Distinct change of color in solution was also observed into brown from dark green. Crystals suitable for X-ray analysis were grown by diffusing pentane over a solution of **7b** in CH_2Cl_2. The coordination sphere around Ru(II) center can be described as a distorted square pyramidal, in which the catalyst possess the uncommon *cis*-dichloro conformation that shows mostly inactive at room temperature.[16] The Ru-O(1) distance of 2.0981(8)Å is in the range observed in ruthenium complexes containing the coordination of ketone functionality.[20]

N-vinylpyrrolidinone reacted even faster with complex **3** under the same condition. Rapid color change to dark brown from bright green was observed within 10 minutes. This was concurrent with the disappearance of the carbene resonance of **3**, along with the appearance of carbene resonance at 13.5 ppm in ^{1}H NMR spectrum. A crystal suitable for X-ray analysis was grown by slow diffusion of pentane to CH_2Cl_2. Crystal structure and representative bond lengths and angles are given in Figure 3, Figure 4, Table 2 and Table 3.

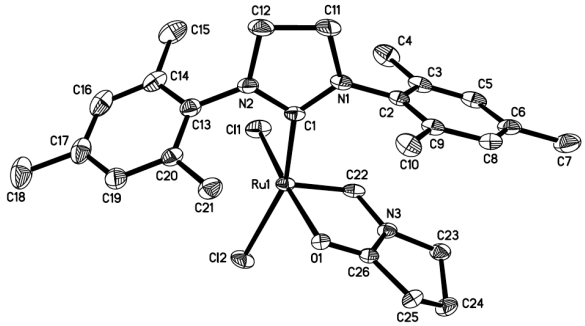

Figure 3. Molecular Structure of Ru complex **7a**

Table 1. Selected bond angles and bond lengths of Ru complex **7a**

Bond Distances(Å)	
Ru-C(1)	1.993(3)
Ru-C(22)	1.816(3)
Ru-O(1)	2.154(2)
Ru-Cl(1)	2.3446(8)
Ru-Cl(2)	2.3786(8)
Bond Angle(deg)	
C(22)-Ru(1)-C(1)	99.44(13)
C(22)-Ru(1)-O(1)	79.80(11)
O(1)-Ru(1)-Cl(1)	173.93(6)
Cl(1)-Ru(1)-Cl(2)	92.42(3)
C(22)-Ru(1)-Cl(1)	94.29(10)
C(1)-Ru(1)-Cl(2)	158.64(9)

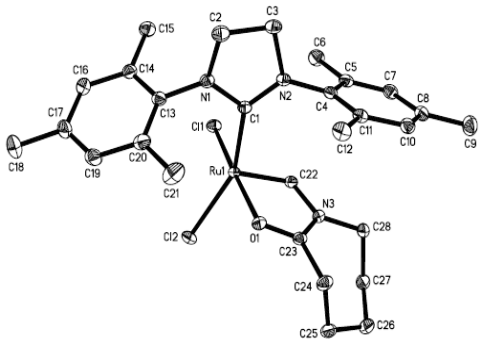

Figure 4. Molecular Structure of Ru complex **7b**

Table 2. Selected bond angles and bond lengths of Ru complex **7b**

Bond Distances(Å)	
Ru-C(1)	1.9929(11)
Ru-C(22)	1.8159(11)
Ru-O(1)	2.0981(8)
Ru-Cl(1)	2.3510(3)
Ru-Cl(2)	2.3729(3)
Bond Angle(deg)	
C(22)-Ru(1)-C(1)	97.61(5)
C(22)-Ru(1)-O(1)	78.75(4)
O(1)-Ru(1)-Cl(1)	173.18(2)
Cl(1)-Ru(1)-Cl(2)	90.132(10)
C(22)-Ru(1)-Cl(1)	95.78(4)
C(1)-Ru(1)-Cl(2)	152.46(3)

Whilst Ru-O(1) bond length of **7a** is 2.154(2) Å, that of **7b** is shorter as 2.0981(8) Å. This difference of bond strength affected their reactivity of olefin metathesis (discussed below). Dependence of Ru-O bond length to ring size could be interpreted by steric of the ring compound. To evaluate chemical effects of steric strains, an effect termed I-strain was suggested for cyclic compounds. Specifically, I-strain refers to change in internal strain of a ring compound which arises from a change in the coordination number and the preferred bond angle of an atom of interest.[21] Both 5- and 7-membered rings are inherently strained to some extent due to the torsional forces about C-C single bonds. Geometrically more flexible caprolactam remains its most stable constellation when chelated compared to the reported crystallographic data of a bare caprolactam.[22] However, chelated pyrrolidinone cannot reduce the sterics around the amide bond as its 5-membered structure is less flexible than 7-membered caprolactam. It is indirectly supported by heats of combustion per methylene group for 5- and 7-membered cyclic alkanes. The reported values are 158.7 and 158.3 kcal/mol for cyclopentane and cycloheptane, respectively.[23] This indicates that 5-membered cyclic compound has slightly higher steric than 7-membered ring. (Simplified model as cyclic alkanes was used because direct comparison of 2-pyrrolidinone and caprolactam is not appropriate as they contain other types of bonds than methylene bonds.) While the angle around amide ketone functionality is close to 130° in complex **7a**, that of complex **7b** is approximately 121°. The more distorted bond prevents carbonyl of complex **7a** from reaching ruthenium center compared to complex **7b**. Hence, the Ru-O bond

length of **7a** becomes longer than that of **7b**. Another interpretation could arise from the enriched electron density of nitrogen. When vinyl lactam coordinates to ruthenium, i.e., after vinyl C-C double bond is replaced with Ru-C bond, nitrogen atom of lactam becomes electron richer. While nitrogen atom of 5-membered ring faces C-H bonds in pseudo-axial position, such steric effect is resolved by chair-like geometry of 7-membered compound. Such repulsion between nitrogen lone pair electron and C-H bond may also distort amide bond to affect ruthenium-carbonyl bond length.

In the NMR spectrum of complex **7a** in CD_2Cl_2, there were always two characteristic peaks at 13.5 and 12.5 ppm. While the major peak of 13.5 ppm was assigned as a carbenic proton, the identity of another was in question. To our surprise, strikingly different NMR spectrum was obtained when NMR spectra was recorded using C_6D_6 as a solvent. Firstly, the major peak was changed from 13.5 ppm to 12.5 ppm, which indicates they could be convertible in a solution phase. In addition, the other protons from NHC backbone and mesitylene group were all appeared as a singlet, unlike the spectrum taken in CD_2Cl_2, in which all protons were split (Figure 5).

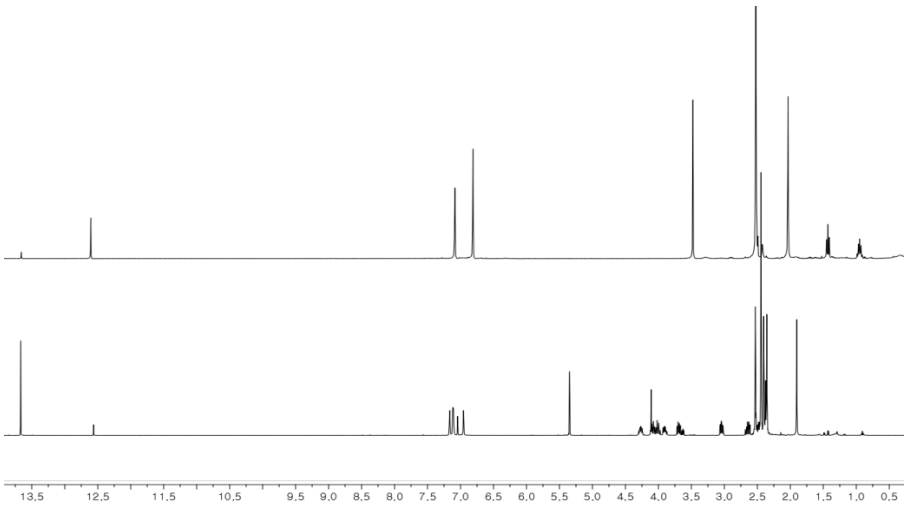

Figure 5. NMR spectrum of complex **7a** in CD_2Cl_2 at 25 °C (below) and C_6D_6 at 75 °C (above)

This phenomenon can be interpreted as a dynamic isomerization between *cis*-dichloro and *trans*-dichloro complexes. When the complex was dissolved in CD_2Cl_2, the isomers exist in 8:1 ratio and the protons for each isomer can be assigned in the spectrum. However, it converts to another isomer almost quantitatively in C_6D_6 at elevated temperature, and shows clear singlet patterns due to its symmetric character and free rotation of the NHC ligand. More interestingly, the unsymmetric nature of *cis*-dichloro isomer influenced the germinal lactam ring protons so that each proton appears separately in the spectrum.

When complex **7b** was dissolved in the same solvents, similar NMR pattern was observed (Table 4). It is postulated that polarity of solvent affects the isomerization since *trans*-dichloro complex has more

symmetric structure. Attempt to dissolve the complex in other solvents such as THF and dioxane was unsuccessful. Isomerization always occurred along with color change of the solution from brown to dark green. Once the majority species are converted from *cis*- to *trans*-dichloro isomer, the ratio didn't restore to the original state, which implicates this isomerization process is non-reversible.

Table 3. Ratio of *cis*- and *trans*-dichloro isomers of **7b**

Solvent	Relative Polarity	Temp. (°C)	Ratio (%*cis*:%*trans*)[a]
CD_2Cl_2	0.309	25	94:6
C_6D_6	0.111	40	59:41
		85	16:84

[a]Measured by NMR

Previously, similar isomerization of sulfur-chelated ruthenium olefin metathesis catalyst induced by UV-light was reported by A. Ben-Asuly et al.[16] In our case, it is believed to be the polarity of solvent influences the isomerization process. The mechanism of such isomerization was suggested to be relocation of the Ru-Cl bonds of 14 electron species followed by dissociation of chelating group.[24]

Reactivity Test. Ring-closing metathesis of diethyldiallyl malonate (DEDAM) was conducted to compare the reactivity of the complexes.

While Complex **7a** showed comparable RCM reactivity at ambient temperature, complex **7b** and had no reactivity at all as shown in Chart 1. This can be explained by the difference of initiation rate which is supported by the shorter Ru-O length of **7a** than that of **7b** as explained in previous section and revealed by their X-ray crystallographic data.

Chart 1. RCM of DEDAM at 25 °C in CD_2Cl_2

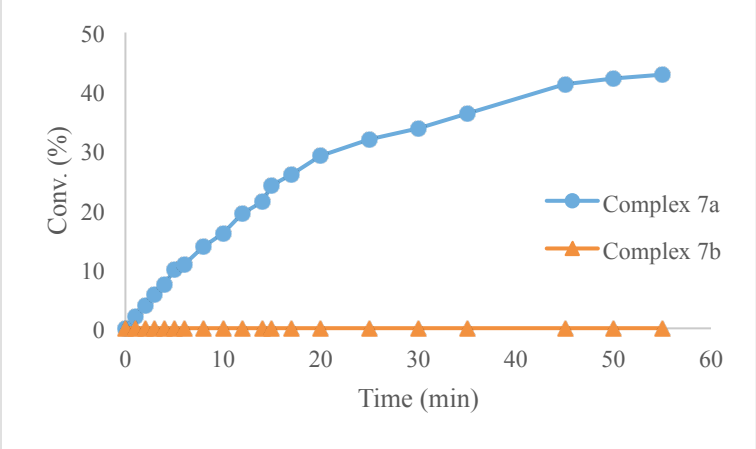

When the reaction temperature was increased to achieve higher conversion, however, unexpected result was achieved. While complex **7a** afforded ring-closed product in >99% conversion within half an hour, complex **7b** catalyzed the reaction very slowly (Chart 2). Moreover, as revealed by its NMR spectra, complex **7b** afforded ring closing metathesis only in minor yield. Rather, it promoted cycloisomerization reaction which is known to be catalyzed by ruthenium hydride species.[25] It is supported by the appearance of the hydride peak in NMR spectra and distinct color change to orange-

yellow which is a representative character of ruthenium hydride species. It was reported that ruthenium-carbene species designed for olefin metathesis could catalyze such reactions in a non-metathetic way.[26,27]

Chart 2. RCM of DEDAM at 85 °C in CD_5CD_3

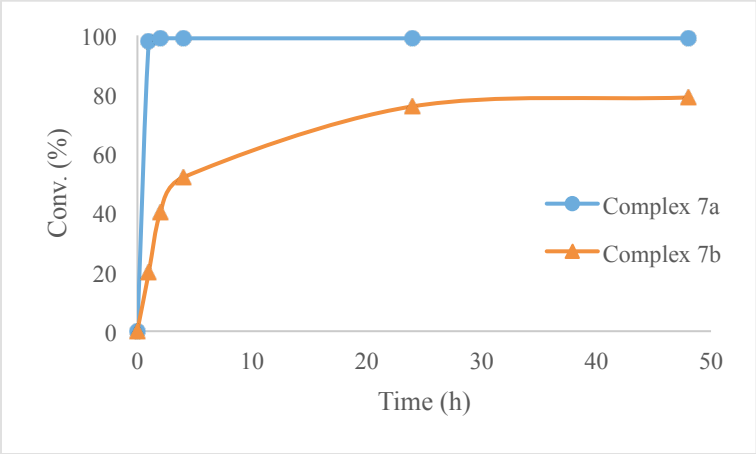

To further study the reaction of complex **7b**, various solvents were tested. The selection of solvent depended on its polarity because the catalyst showed structural difference when the solvent varied. The ratio of RCM and cycloisomerization products highly depends on solvents (Table 1). Polar solvent such as dichloromethane didn't afford any product for both reaction, but less polar benzene gave cycloisomerization product in 84% yield along with 4.8 of RCM yield (Entry 4). When the polar solvent with higher boiling point, for example, dichloroethane or tetrachloroethane was used to increase the reaction temperature, ring-closing metathesis was dominant but the yield was poor (Entry 7, 27%).

Table 4. RCM versus cycloisomerization depending on the solvent

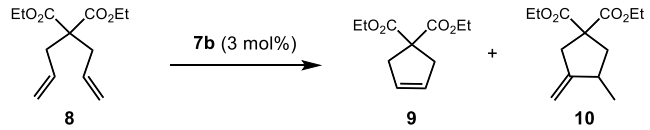

8 9 10

Entry	Solvent	Temp. (°C)	Time (h)	Yield of 9 (%)[a]	Yield of 10 (%)[a]
1	CD_2Cl_2	25	1	0	0
2	CD_2Cl_2	40	24	0	0
3	C_6D_6	85	1	<1	29
4	C_6D_6	85	48	4.8	84
5	$C_2D_4Cl_2$	75	22	3.6	36
6	$C_2D_2Cl_4$	75	7	0	0
7	$C_2D_2Cl_4$	120	24	27	7

[a]Measured by NMR;

Conclusion

In an attempt to develop a novel ruthenium olefin metathesis catalyst, two complexes with chelating *N*-vinyl lactam were synthesized. It was expected that the combination of electron donating effect of nitrogen atom adjacent to the carbenic carbon and labile carbonyl chelation would afford highly reactive metathesis catalysts with its stability remained. However, the complexes didn't show greater olefin metathesis reactivity compared to the commercially available ruthenium olefin metathesis catalysts. 5-membered lactam ligand afforded comparably reactive catalyst. 7-membered lactam-coordinated complex was unreactive toward olefin metathesis, however, upon thermal stimuli it catalyzed cycloisomerization reaction in a high yield. Another interesting feature of the complexes was that it showed *cis*- and *trans*-dichloro isomerization behavior depending on the polarity of the solvent.

This study showed that *N*-vinyl lactam can be used as a ligand for olefin metathesis catalysts. Combination of chelating property of carbonyl group and electron-richness of ruthenium center induced by Fischer carbene can pave a new way in olefin metathesis catalyst development. It is expected that further study by varying electronic property of the chelating ligand would result highly effective catalysts.

Experimental Section

Compound **7a**: *N*-vinyl caprolactam (0.24 mmol) and second generation Grubbs catalyst (0.12 mmol) were dissolved in dichloromethane (5 mL) in a 10 mL schlenk tube. The reaction mixture was stirred at room temperature for 5 h. The resulting mixture was filtered through celite, then concentrated to 2-3 mL dichloromethane. After the reaction, CH_2Cl_2 was reduced to minimal amount and recrystallization in diethylether followed by washing with pentane gave the product (60%). Crystals suitable for X-ray were obtained by slow diffusion between pentane and a solution of **2** in dichloromethane. ^{1}H NMR (CD_2Cl_2, 400 MHz) : δ 13.41 (s, 1H), 7.11-6.88 (m, 4H), 4.20-4.16 (m, 1H), 3.97-3.78 (m, 3H), 3.47-3.39 (m, 2H), 2.97-2.92 (m, 1H), 2.60-2.30 (m, 16H), 1.88-1.72 (m, 6H), 1.50-1.30 (m, 3H) ^{13}C NMR (CD_2Cl_2, 100 MHz) : 217.1, 185.2, 139.9, 139.8, 138.9, 138.6, 137.8, 135.5, 131.8, 131.5, 130.1, 129.8, 129.3, 128.7, 55.5, 53.9, 51.0, 34.5, 29.6, 27.9, 23.2, 21.0, 19.6, 18.0, 17.9, 16.9.

Compound **7b**: 1-vinyl-2-pyrrolidinone (0.24 mmol), cuprous chloride (0.12 mmol) and second generation Grubbs catalyst (0.12 mmol) were dissolved in dichloromethane (5 mL) in a 10 mL schlenk tube. The reaction mixture was stirred at room temperature for 3 h. (The consumption of second generation Grubbs catalyst was monitored by ^{1}H NMR). The resulting mixture was filtered through celite, then

concentrated to 2-3mL dichloromethane. Crude product was purified by recrystallization in diethylether followed by washing with pentane to afford the desired product. Recrystallization from a mixture pentane and dichloromethane afforded **7b**, as maroon crystals in 40 % yield. ^{1}H NMR (CD_2Cl_2, 400 MHz) :δ 13.50 (s, 1H), 6.98 (s, 2H), 6.88 (s, 2H), 3.96 (m, 4H), 2.43-2.44 (ss, 18H), 2.12-2.03 (m, 2H), 3.51 (m, 1H), 2.92 (m, 1H), 1.77-1.64 (m, 2H) ^{13}C NMR (CD_2Cl_2, 100 MHz) : 216.7, 185.9, 139.2, 138.8, 138.6, 138.4, 138.0, 136.4, 136.3, 131.1, 130.0, 129.4, 128.8, 125.2, 124.9, 123.8, 51.1, 46.9, 31.0, 27.6, 27.2, 26.0, 22.9, 20.9, 17.9.

General procedure for RCM reactions. Typically 5 mol % of the catalyst was added to a solution of substrate (0.10 mmol) using capped NMR tube in 0.5 ml of deuterated solvent. When necessary, the reaction was heated in the NMR probe and analyzed by arrayed experiment.

Reference

(1) *Handbook of Metathesis*; Grubbs, R. H. ed.; Wiley-VCH: Weinhein, Germany, 2003.

(2) *Olefin Metathesis: Theory and Practice*; Grela, Karol ed.; John Wiley & Sons: Hoboken, New Jersey, 2014.

(3) Hoveyda, A. H.; Zhugralin, A. R. *Nature* **2007**, *450*, 243.

(4) Trnka, T. M.; Grubbs, R. H. *Acc. Chem. Res.* **2000**, *34*, 18.

(5) Schrock, R. R.; Hoveyda, A. H. *Angew. Chem. Int. Ed.* **2003**, *42*, 4592.

(6) Vougioukalakis, G. C.; Grubbs, R. H. *Chem. Rev.* **2010**, *110*, 1746.

(7) Scholl, M.; Ding, S.; Lee, C. W.; Grubbs, R. H. *Organic Letters* **1999**, *1*, 953.

(8) Garber, S. B.; Kingsbury, J. S.; Gray, B. L.; Hoveyda, A. H. *J. Am. Chem. Soc.* **2000**, *122*, 8168.

(9) Michrowska, A.; Bujok, R.; Harutyunyan, S.; Sashuk, V.; Dolgonos, G.; Grela, K. *J. Am. Chem. Soc.* **2004**, *126*, 9318.

(10) Tzur, E.; Szadkowska, A.; Ben-Asuly , A.; Makal, A.; Goldberg, I.; Woźniak, K.; Grela , K.; Lemcoff, N. G. *Chemistry – A European Journal* **2010**, *16*, 8726.

(11) Slugovc, C.; Perner, B.; Stelzer, F.; Mereiter, K. *Organometallics* **2004**, *23*, 3622.

(12) Slugovc, C.; Burtscher, D.; Stelzer, F.; Mereiter, K. *Organometallics* **2005**, *24*, 2255.

(13) Fürstner, A.; Thiel, O. R.; Lehmann, C. W. *Organometallics* **2001**, *21*, 331.

(14) Hejl, A.; Day, M. W.; Grubbs, R. H. *Organometallics* **2006**, *25*, 6149.

(15) Hansen, S. M.; Volland, M. A. O.; Rominger, F.; Eisenträger, F.; Hofmann, P. *Angew. Chem. Int. Ed.* **1999**, *38*, 1273.

(16) Ben-Asuly, A.; Aharoni, A.; Diesendruck, C. E.; Vidavsky, Y.; Goldberg, I.; Straub, B. F.; Lemcoff, N. G. *Organometallics* **2009**, *28*, 4652.

(17) Louie, J.; Grubbs, R. H. *Organometallics* **2002**, *21*, 2153.

(18) Wu, Z.; Nguyen, S. T.; Grubbs, R. H.; Ziller, J. W. *J. Am. Chem. Soc.* **1995**, *117*, 5503.

(19) Thomas, R. M.; Fedorov, A.; Keitz, B. K.; Grubbs, R. H. *Organometallics* **2011**, *30*, 6713.
(20) Dixneuf, P. H.; Romero, A.; Vegas, A. *Angew. Chem., Int. Ed.* **1990**, *29*, 215.
(21) Brown, H. C.; Gerstein, M. *J. Am. Chem. Soc.* **1950**, *72*, 2926.
(22) Oya, K. P.; Myasnikova, R. M. *J. Struct. Chem.* **1974**, *15*, 578.
(23) Spitzer, R.; Huffman, H. M. *J. Am. Chem. Soc.* **1947**, *69*, 211.
(24) Barbasiewicz, M.; Szadkowska, A.; Bujok, R.; Grela, K. *Organometallics* **2006**, *25*, 3599.
(25) Yamamoto, Y.; Nakagai, Y.-i.; Ohkoshi, N.; Itoh, K. *J. Am. Chem. Soc.* **2001**, *123*, 6372.
(26) Schmidt, B. *Eur. J. Org. Chem.* **2004**, *2004*, 1865.
(27) Terada, Y.; Arisawa, M.; Nishida, A. *Angew. Chem. Int. Ed.* **2004**, *43*, 4063.

Supplementary Information

Table of Contents

1. Method and Materials

All reactions were carried out using standard Schlenk techniques, or in an argon-filled glove box unless otherwise mentioned. Deuterated solvents were dried under the calcium hydride and vacuum transferred prior to use. NMR spectra were obtained on an Agilent 400-MR DD2 Magnetic Resonance System (400 MHz). Chemical shift values were recorded in ppm relative to tetramethylsilane (TMS) as an internal standard, and coupling constants in Hertz (Hz). Grubbs catalyst second generation was purchased from Sigma-Aldrich. Most substrates were obtained from commercial suppliers and used as received without further purification.

2. Spectra

Complex 7a

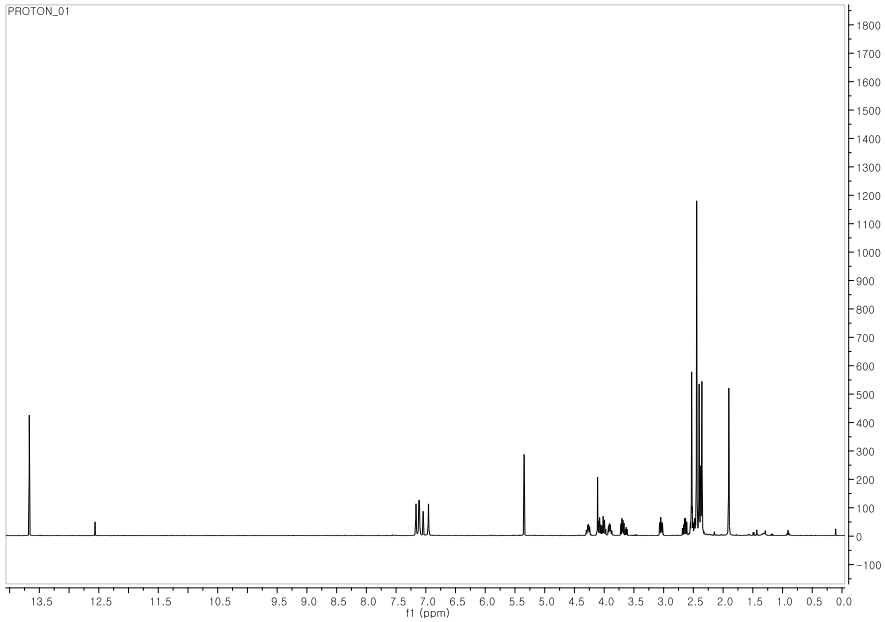

^{1}H NMR (500 MHz, CD_2Cl2) mixture of *cis*-dichloro and *trans*-dichloro complexes (ratio 8:1)
***cis*-dichloro** δ 13.65 (s, 1H), 7.14 (s, 1H), 7.09 (d, *J* = 5.1 Hz, 2H), 6.95 (d, *J* = 14.8 Hz, 1H), 4.35 – 4.21 (m, 1H), 4.10 – 3.95 (m, 2H), 3.89 (dd, *J* = 10.6,

5.9 Hz, 1H), 3.69 – 3.64 (m, 1H), 3.04 – 2.99 (dt, 1H), 2.66 – 2.58 (m, 1H), 2.50 (s, 3H), 2.42 (s, 6H), 2.38 (s, 3H), 2.33 (s, 3H), 1.88 (s, 3H)

***trans*-dichloro** δ 12.54 (s, 1H), 7.02 (s, 4H), 4.09 (s, 4H), 3.61 (t, 2H), 2.50 – 2.43 (m, 2H), 2.42 (s, 6H), 2.35 (s, 12H)

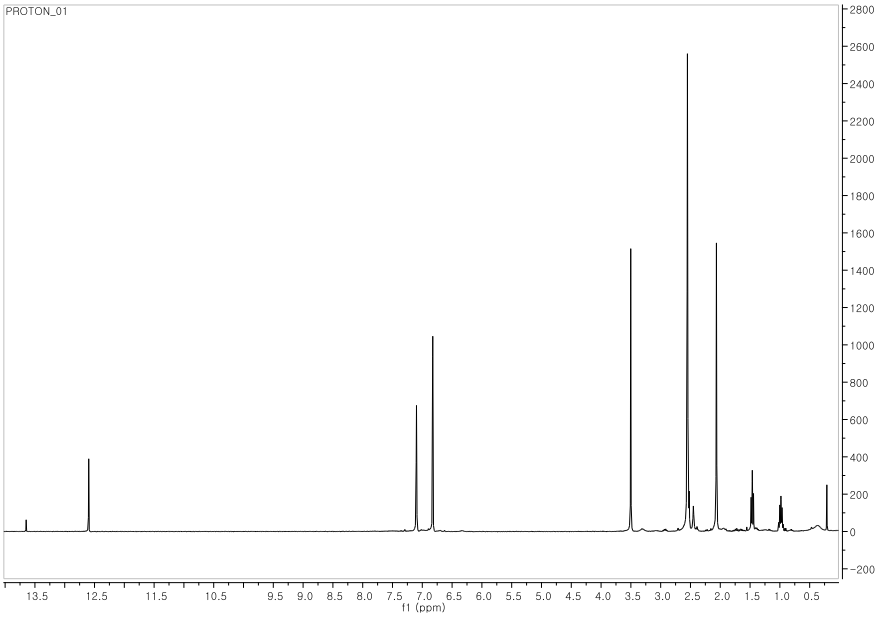

^{1}H NMR (400 MHz, C_6D_6, 75 °C) δ 12.66 (s, 4H), 6.89 (s, 4H), 3.57 (s, 4H), 2.60 (s, 12H), 2.13 (s, 6H), 1.59 – 1.45 (m, 2H), 1.14 – 0.98 (m, 2H).

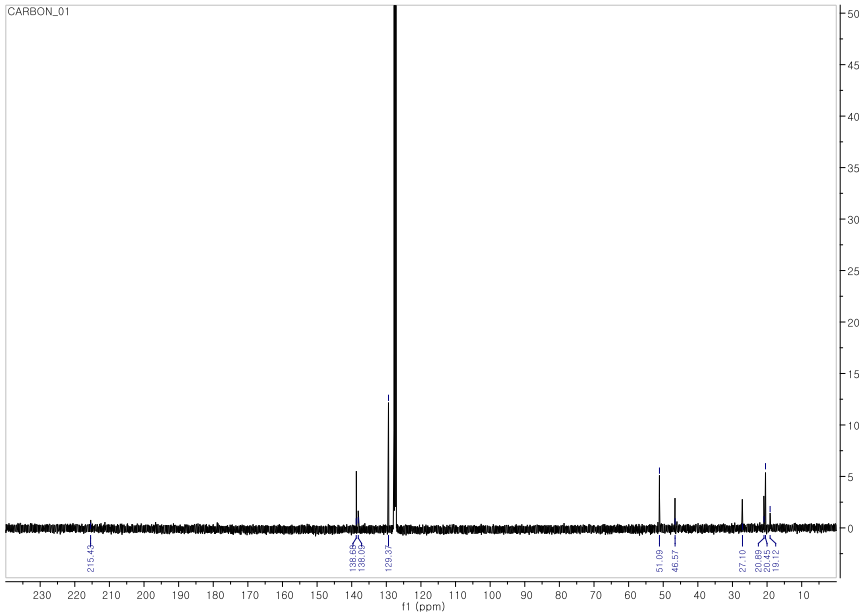

^{13}C NMR (100 MHz, C_6D_6) δ 215.43, 138.68, 138.09, 129.37, 51.09, 46.57, 27.15, 20.89, 20.45, 19.12.

Complex 7b

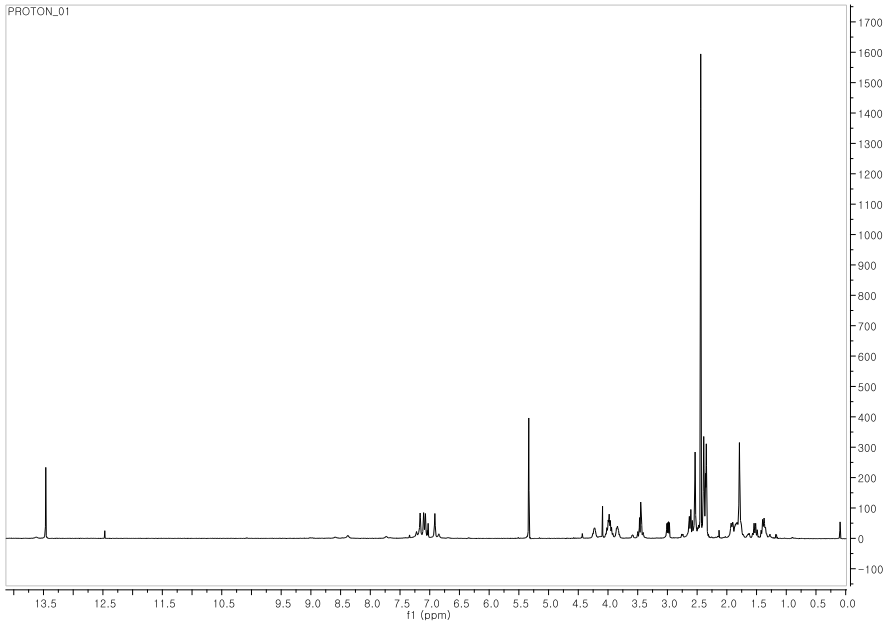

^{1}H NMR (500 MHz, CD_2Cl2) *cis*-dichloro as large majority
δ 13.46 (s, 1H), 7.27 – 7.03 (m, 3H), 6.88 (d, *J* = 33.3 Hz, 1H), 4.27 – 4.11 (m, 1H), 4.07 – 3.80 (m, 2H), 3.78-3.75 (m, 1H), 3.44 (dd, *J* = 22.6, 7.9 Hz, 1H), 2.99 (dd, *J* = 14.0, 7.1 Hz, 1H), 2.72 – 1.31 (m, 26H)

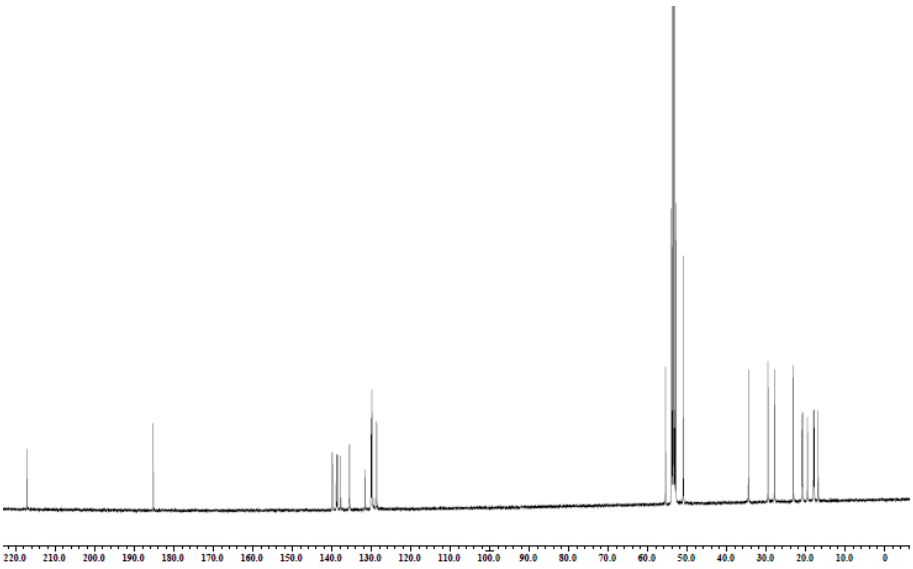

^{13}C NMR (100 MHz, CD_2Cl_2) 216.7, 185.9, 139.2, 138.8, 138.6, 138.4, 138.0, 136.4, 136.3, 131.1, 130.0, 129.4, 128.8, 125.2, 124.9, 123.8, 51.1, 46.9, 31.0, 27.6, 27.2, 26.0, 22.9, 20.9, 17.9.

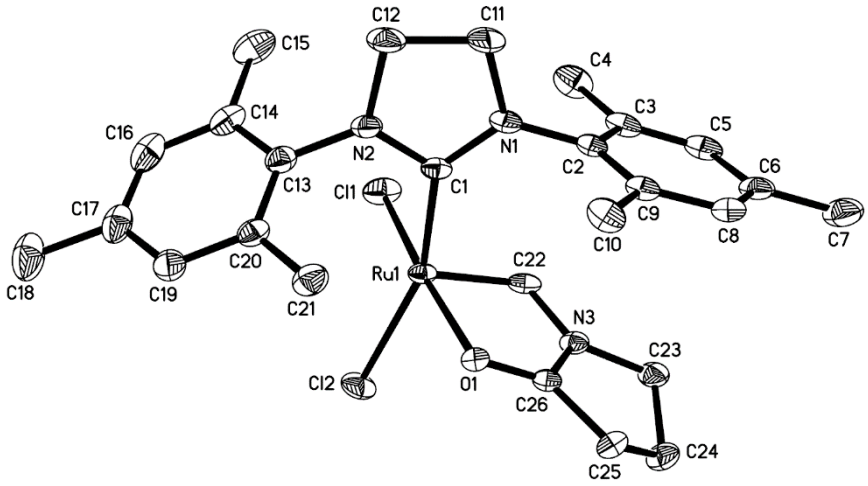

F**igure S1.** Molecular structure of complex **7a**.

Table S1. Crystal data and structure refinement for complex **7a**.

Identification code	hsh61	
Empirical formula	C27 H35 Cl4 N3 O Ru	
Formula weight	660.45	
Temperature	103(2) K	
Wavelength	0.71073 Å	
Crystal system	Triclinic	
Space group	P-1	
Unit cell dimensions	a = 11.8364(4) Å	α= 71.9080(10)°.
	b = 15.0197(5) Å	β= 89.1890(10)°.
	c = 17.3630(5) Å	γ = 77.9660(10)°.
Volume	2865.43(16) $Å^3$	
Z	4	
Density (calculated)	1.531 Mg/m^3	
Absorption coefficient	0.946 mm^{-1}	
F(000)	1352	
Crystal size	0.40 x 0.40 x 0.38 mm^3	
Theta range for data collection	1.24 to 31.08°.	

Index ranges	-17<=h<=17, -21<=k<=21, -25<=l<=19
Reflections collected	80314
Independent reflections	18200 [R(int) = 0.0398]
Completeness to theta = 31.08°	98.9 %
Absorption correction	Semi-empirical from equivalents
Max. and min. transmission	0.7151 and 0.7035
Refinement method	Full-matrix least-squares on F^2
Data / restraints / parameters	18200 / 106 / 689
Goodness-of-fit on F^2	1.073
Final R indices [I>2sigma(I)]	R1 = 0.0478, wR2 = 0.1264
R indices (all data)	R1 = 0.0646, wR2 = 0.1459
Largest diff. peak and hole	2.527 and -2.322 e.$Å^{-3}$

Table S1. Selected bond lengths (Å) and angles (°) for complex **7a**.

Ru(1)-C(22)	1.816(3)	C(22)-Ru(1)-C(1)	99.44(13)
Ru(1)-C(1)	1.993(3)	C(22)-Ru(1)-O(1)	79.80(11)
Ru(1)-O(1)	2.154(2)	C(1)-Ru(1)-O(1)	95.66(10)
Ru(1)-Cl(1)	2.3446(8)	C(22)-Ru(1)-Cl(1)	94.29(10)
Ru(1)-Cl(2)	2.3786(8)	C(22)-Ru(1)-Cl(2)	101.91(9)
C(22)-N(3)	1.382(4)	C(1)-Ru(1)-Cl(2)	158.64(9)
C(22)-H(22)	0.9500	O(1)-Ru(1)-Cl(2)	87.44(6)
C(19)-H(19)	1.513(5)	Cl(1)-Ru(1)-Cl(2)	92.42(3)
C(23)-N(3)	1.476(4)	N(3)-C(22)-Ru(1)	116.4(2)
C(23)-C(24)	1.538(5)	N(3)-C(22)-H(22)	121.8
C(23)-H (23A)	0.9900	N(3)-C(23)-C(24)	101.6(3)
C(23)-H(23B)	0.9900	C(25)-C(24)-C(23)	105.1(3)
C(24)-C(25)	1.532(4)	C(26)-C(25)-C(24)	101.8(3)
C(24)-H(24A)	0.9900	O(1)-C(26)-N(3)	119.3(3)
C(24)-H(24B)	0.9900	O(1)-C(26)-C(25)	130.4(3)
C(25)-C(26)	1.494(4)	N(3)-C(26)-C(25)	110.3(3)
C(25)-H(25A)	0.9900	C(26)-N(3)-C(22)	115.3(3)
C(25)-H(25B)	0.9900	C(22)-N(3)-C(23)	132.0(3)
C(26)-O(1)	1.252(4)		
C(26)-N(3)	1.350(4)		

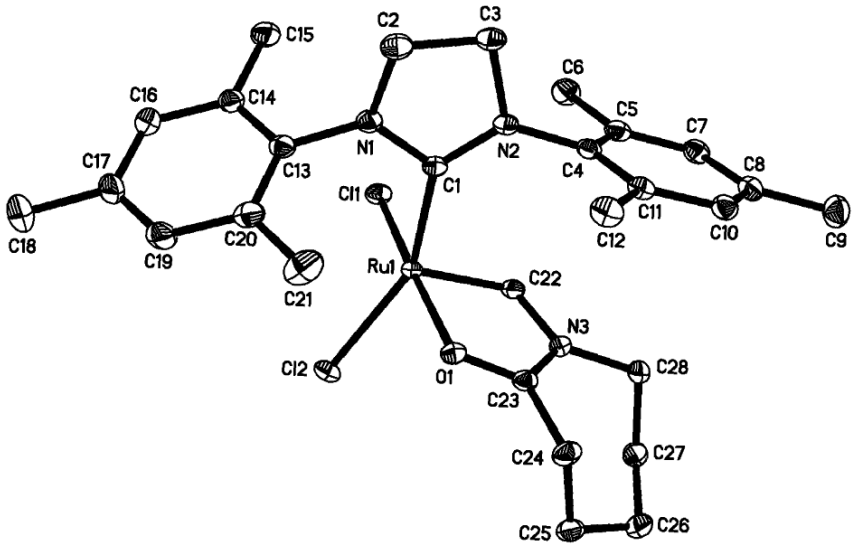

Figure S2. Molecular structure of complex **7b**.

Table S3. Crystal data and structure refinement for complex **7b**.

Identification code	hsh54s	
Empirical formula	C29 H39 Cl4 N3 O Ru	
Formula weight	688.50	
Temperature	103(2) K	
Wavelength	0.71073 Å	
Crystal system	Monoclinic	
Space group	P2(1)/c	
Unit cell dimensions	a = 11.6929(3) Å	α= 90°.
	b = 12.7939(3) Å	β= 104.8350(10)°.
	c = 21.9609(5) Å	γ = 90°.
Volume	3175.79(13) $Å^3$	
Z	4	
Density (calculated)	1.440 Mg/m^3	
Absorption coefficient	0.857 mm^{-1}	
F(000)	1416	
Crystal size	0.40 x 0.40 x 0.14 mm^3	

Theta range for data collection	2.49 to 34.12°.
Index ranges	-17<=h<=18, -20<=k<=19, -34<=l<=33
Reflections collected	53589
Independent reflections	13041 [R(int) = 0.0298]
Completeness to theta = 34.12°	99.6 %
Absorption correction	Semi-empirical from equivalents
Max. and min. transmission	0.8895 and 0.7257
Refinement method	Full-matrix least-squares on F^2
Data / restraints / parameters	13041 / 0 / 349
Goodness-of-fit on F^2	1.033
Final R indices [I>2sigma(I)]	R1 = 0.0247, wR2 = 0.0599
R indices (all data)	R1 = 0.0311, wR2 = 0.0631
Largest diff. peak and hole	0.975 and -0.865 e.$Å^{-3}$

Table S4. Selected bond lengths (Å) and angles (°) for complex **7b**.

Ru(1)-C(22)	1.8159(11)	C(22)-Ru(1)-C(1)	97.61(5)
Ru(1)-C(1)	1.9929(11)	C(22)-Ru(1)-O(1)	78.75(4)
Ru(1)-O(1)	2.0981(8)	C(1)-Ru(1)-O(1)	95.51(4)
Ru(1)-Cl(1)	2.3510(3)	C(22)-Ru(1)-Cl(1)	95.78(4)
Ru(1)-Cl(2)	2.3729(3)	C(1)-Ru(1)-Cl(1)	89.21(3)
C(22)-N(3)	1.3924(14)	O(1)-Ru(1)-Cl(1)	173.18(2)
C(22)-H(22)	0.9500	C(22)-Ru(1)-Cl(2)	109.84(3)
C(23)-O(1)	1.2540(14)	C(1)-Ru(1)-Cl(2)	152.46(3)
C(23)-N(3)	1.3555(15)	O(1)-Ru(1)-Cl(2)	87.95(2)
C(23)-C(24)	1.4908(16)	Cl(1)-Ru(1)-Cl(2)	90.132(10)
C(24)-C(25)	1.5402(17)	N(3)-C(22)-Ru(1)	118.18(8)
C(24)-H(24A)	0.9900	N(3)-C(22)-H(22)	120.90
C(24)-H(24B)	0.9900	Ru(1)-C(22)-H(22)	120.90
C(25)-C(26)	1.527(2)	O(1)-C(23)-N(3)	117.26(10)
C(25)-H(25A)	0.9900	O(1)-C(23)-C(24)	121.53(11)
C(25)-H(25B)	0.9900	N(3)-C(23)-C(24)	121.13(10)
C(26)-C(27)	1.527(2)	C(23)-C(24)-C(25)	111.19(9)
C(26)-H(26A)	0.9900	C(26)-C(25)-C(24)	114.64(10)
C(26)-H(26B)	0.9900	C(25)-C(26)-C(27)	116.22(10)
C(27)-C(28)	1.5234(17)	C(28)-C(27)-C(26)	114.49(11)
C(27)-H(27A)	0.9900	N(3)-C(28)-C(27)	112.55(10)
C(27)-H(27B)	0.9900		
C(28)-N(3)	1.4754(15)		
C(28)-H(28A)	0.9900		
C(28)-H(28B)	0.9900		

요약문

올레핀 메타테시스 반응은 탄소간의 이중 결합을 재배치하여 새로운 이중 결합 분자를 형성하는 반응이다. 이 반응에는 루테늄, 텅스텐, 몰리브데늄 등의 금속 촉매가 널리 알려져 있으며, 특히 루테늄 촉매는 공기 또는 수분과의 접촉에 다른 금속보다 덜 민감하므로 유기화학 분야에서 널리 사용되고 있다. 본 연구에서는 *N*-비닐 락탐을 리간드로 사용하여 전자밀도가 풍부한 금속 중심 원자를 지님과 동시에 락탐의 키톤기가 금속 중심 원자에 배위하여 빠른 초기 속도를 가지도록 촉매 구조를 고안하였다. 다른 고리 크기를 가진 두 종류의 락탐을 이용하여 촉매를 합성하였을 때, 기대한 바와 같이 메타테시스 반응성이 관찰되긴 하였으나 상용화된 촉매들보다 우수하지 않은 수율을 나타내었다. 반응성을 증대시키기 위해 고온에서 반응을 진행하면 메타테시스 수율은 낮아지고 고리이성질화 반응을 촉매하였으며, 반응의 최대 수율은 84%이다. 또한 본 연구에서 합성된 촉매는 용매의 극성에 따라 용액 상에서 시스-디클로로 또는 트랜스-디클로로 구조를 갖는다. 이러한 구조 변화는 기존 연구에서 종종 보고되었으나, 용매에 의존하여 이성질화가 이루어지는 것은 드물게 관찰되지 않았던 특징이다.

본 연구를 통해 *N*-비닐 락탐이 올레핀 메타테시스 촉매의 리간드로 사용될 수 있음을 보였다. 키톤기의 배위, 피셔 카빈에서 기인하는 전자가 풍부한 루테늄 등의 특징이 새로운 형태의 메타테시스 촉매 개발을 가능하게 하였다. 리간드로 사용되는 아마이드의 전자적 성질을 변화시키는 차후 연구를 통해 이러한 촉매의 반응성의 증대가 기대된다.

이학석사학위논문

Ruthenium Olefin Metathesis Catalysts Bearing Chelating *N*-Vinyl Lactam Ligands: Synthesis, Structure, and Reactivity

N-비닐 락탐 배위 루테늄 올레핀 메타테시스 촉매의 합성, 구조 및 반응성 연구

2015 년 8 월

서울대학교 대학원

화학부 유기화학 전공

김 민 하

Abstract

Ruthenium Olefin Metathesis Catalysts Bearing Chelating *N*-Vinyl Lactam Ligands: Synthesis, Structure, and Reactivity

Min Ha Kim
Department of Chemistry
The Graduate School
Seoul National University

Novel, phosphine-free ruthenium carbene complexes with carbonyl-chelating lactam ligand were synthesized. X-ray crystallography confirmed intramolecular coordination of pendant carbonyl group. Highly electron donating nature of Fischer carbenes induced great stability to the compounds. The complexes could catalyze olefin metathesis and cycloisomerization reaction depending on solvent and temperature conditions. Additionally, their structural peculiarity of *cis*- and *trans*-dichloro geometry was studied by NMR analysis.

Keywords **:** Olefin metathesis, ruthenium, organometallics, catalysis, cycloisomerization, carbene

Student Number : 2013-22917

Table of Contents

List of Figures

List of Schemes

List of Charts

List of Tables

Introduction

In recent decades, olefin metathesis emerged as a versatile tool for organic synthesis and polymer chemistry.[1-3] It is a unique carbon-carbon bond formation reaction which redistributes the fragments of alkenes across the double bond to furnish partner-changed olefins via metallacyclobutane intermediate. The evolution of this methodology was accelerated after the development of well-defined Ru, Mo, and W catalysts and study of mechanism.[4,5] Among a variety of the catalysts, ruthenium carbene complexes are especially advantageous because they are less sensitive toward air and moisture with their high reactivity and selectivity remained.[6] Development of modern ruthenium olefin metathesis catalysts has been aimed at increasing their selectivity as well as reactivity by modification of structure.

The first breakthrough in catalyst development was achieved by replacement of one phosphine ligand by *N*-heterocyclic carbene (NHC), which led to the second generation ruthenium olefin metathesis catalyst (complex 1, Figure 1).[7] This complex exhibits distinctly higher reactivity and functional group tolerance compared to its parental bisphosphine first generation complex. Soon after, chelation of styrenyl ether resulted Hoveyda-type complexes, of which their stability were highly improved (complex 2, Figure 1).[8] As the Hoveyda-type complexes proved, additional chelation to the metal center contributes to thermal, air, and moisture stability. Although

various chelated ruthenium alkylidene complexes were reported to be sufficiently reactive, most of the chelating ligands suffer from tedious synthetic problems. Such drawbacks also hindered the systematic study of electronic variation of the ligands, which is valuable for development of more efficient catalysts.[9,10] While the stability is increased adopting chelation of styrenyl ether moiety, fast initiation was achieved by replacing the phosphine ligand with more labile ligands (complex 3, Figure 1). Fast initiation is crucial for polymer synthesis since the initial reaction rate affects the important characters of the polymeric product, for example, average molecular weight or polydispersity index.

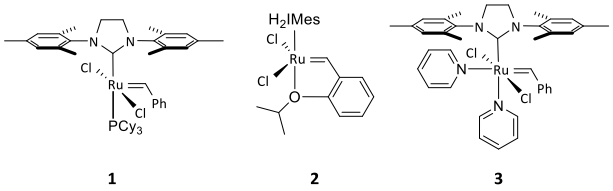

Figure 1. Commonly used Ru olefin metathesis catalysts

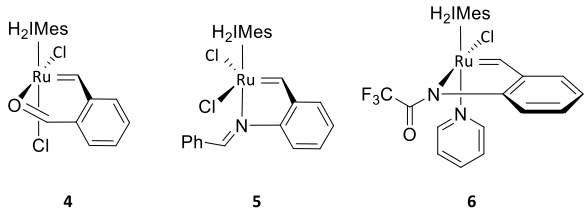

Figure 2. Selected examples of *N*- and *O*-chelated Ru olefin metathesis catalysts[11-14]

Chelated Ru carbene complexes with various electron-donating ligands were reported, and the representative examples are shown in Figure 2. In most cases, supplementary coordination resulted stabilization, or even latency to the catalysts.

Most of the well-defined ruthenium olefin metathesis catalysts have a square-pyramidal coordination of Ru center with *trans*-halido geometry.[15] In 1999, Hoffmann et al. reported one exceptional example, which was triggered by chelating bisphosphine ligand. In such complexes, P-Ru-Cl *trans* (i.e. Cl-Ru-Cl *cis*) arrangement was forced. Since the dissociation of the neutral ligand is required for the initiation of the catalytic cycle, appropriate design of this leaving ligand can accelerate or retard the initiation rate. Control of the initiation rate is of high interest for chemists since it often provides a clue for the entire reaction time. Especially in polymer chemistry, polymer with even distribution of molecular weight can only be obtained under the initiation in an instant. This is usually achieved by utilizing so-called latent catalysts, which are activated by external stimuli such as thermal, photo, or chemical treatment.[16]

Amide bonds are ubiquitous in both nature and chemical industry, for example, it is a key structural unit in peptides and one of the most pervasive source for polymers. Since amides contain carbonyl group which can coordinate to the metal center, they can be considered as a suitable candidate as a chelating ligand. The comprehensive study of complexes with electron-rich carbenes such as ethyl vinyl ether, vinyl sulfide, *N*-vinyl carbazole, and *N*-vinyl pyrrolidinone was conducted by Grubbs and co-worker.[17] Whilst such Fischer-type Ru complexes

had been reported to be relatively inert toward olefin metathesis reactions,[18] comparable reactivity was observed for some series of the complexes. Interestingly, it was reported that intramolecular coordination of the amide carbonyl group was detected in the ^{1}H NMR spectrum.[17,19]

Inspired by the combination of strongly electron donating character of Fischer carbene and carbonyl chelation which could result balance in stability and reactivity, we aimed at synthesis of ruthenium olefin metathesis catalysts with chelating *N*-vinyl lactam ligands. Herein, we report the synthesis, characterization, and reactivity of the complexes.

Results and Discussion

Catalyst Synthesis. The catalysts were synthesized from readily available *N*-vinyl lactams. The first attempts to synthesize lactam-chelated complex via reaction of phosphine-containing complex (1) didn't afford the products clearly. From the in situ NMR study of the reaction between complex 1 and vinyl lactam, we could observe that phosphine remained in the mixture. Although 1.1 to 1.5 equivalence of copper (I) chloride was added to thoroughly remove phosphine residue, chelated phosphine-free complex was not affordable. Inspired by lability of pyridine ligand, problematic phosphine ligand was replaced with pyridine. Finally, successful synthesis of lactam-chelated complexes as pale grey solid was achieved (Scheme 1). Products were purified by recrystallization in diethyl ether and yields were 60% (7a) or 40% (7b). Attempts to increase the yield by driving the equilibrium using large equivalence of lactam (up to 5 equiv.) resulted slightly negative effect due to excess amount of diethyl ether used during washing.

Scheme 1. Synthesis of catalysts with *N*-vinyl amides

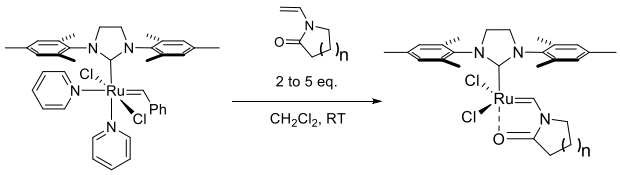

3 **7**
(**7a**: n=1, **7b**: n=3)

Characterization and Structural Peculiarity. Substitution reaction of complex **3** using commercially available *N*-vinylcaprolactam was performed (Scheme 1) to afford complex **7b.** To monitor the formation progress of chelated Fischer carbene complex, ^{1}H NMR was employed using characteristic chemical shift of the carbonic proton, from which 19.0 ppm from **3** was completely disappeared concomitant appearance of 13.4 ppm in the formation of complex **7b** after 3 hours. Distinct change of color in solution was also observed into brown from dark green. Crystals suitable for X-ray analysis were grown by diffusing pentane over a solution of **7b** in CH_2Cl_2. The coordination sphere around Ru(II) center can be described as a distorted square pyramidal, in which the catalyst possess the uncommon *cis*-dichloro conformation that shows mostly inactive at room temperature.[16] The Ru-O(1) distance of 2.0981(8)Å is in the range observed in ruthenium complexes containing the coordination of ketone functionality.[20]

N-vinylpyrrolidinone reacted even faster with complex **3** under the same condition. Rapid color change to dark brown from bright green was observed within 10 minutes. This was concurrent with the disappearance of the carbene resonance of **3**, along with the appearance of carbene resonance at 13.5 ppm in ^{1}H NMR spectrum. A crystal suitable for X-ray analysis was grown by slow diffusion of pentane to CH_2Cl_2. Crystal structure and representative bond lengths and angles are given in Figure 3, Figure 4, Table 2 and Table 3.

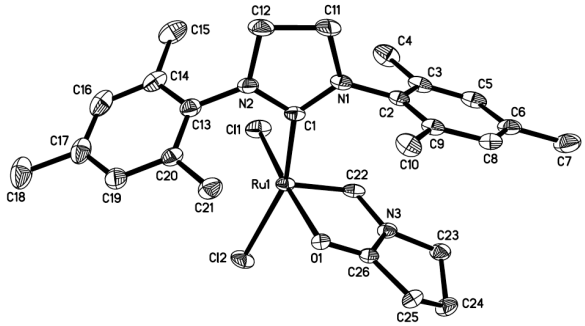

Figure 3. Molecular Structure of Ru complex **7a**

Table 1. Selected bond angles and bond lengths of Ru complex **7a**

Bond Distances(Å)	
Ru-C(1)	1.993(3)
Ru-C(22)	1.816(3)
Ru-O(1)	2.154(2)
Ru-Cl(1)	2.3446(8)
Ru-Cl(2)	2.3786(8)
Bond Angle(deg)	
C(22)-Ru(1)-C(1)	99.44(13)
C(22)-Ru(1)-O(1)	79.80(11)
O(1)-Ru(1)-Cl(1)	173.93(6)
Cl(1)-Ru(1)-Cl(2)	92.42(3)
C(22)-Ru(1)-Cl(1)	94.29(10)
C(1)-Ru(1)-Cl(2)	158.64(9)

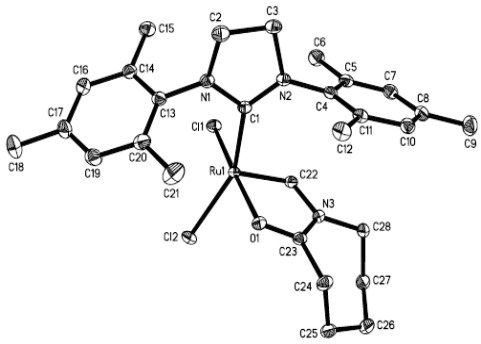

Figure 4. Molecular Structure of Ru complex **7b**

Table 2. Selected bond angles and bond lengths of Ru complex **7b**

Bond Distances(Å)	
Ru-C(1)	1.9929(11)
Ru-C(22)	1.8159(11)
Ru-O(1)	2.0981(8)
Ru-Cl(1)	2.3510(3)
Ru-Cl(2)	2.3729(3)
Bond Angle(deg)	
C(22)-Ru(1)-C(1)	97.61(5)
C(22)-Ru(1)-O(1)	78.75(4)
O(1)-Ru(1)-Cl(1)	173.18(2)
Cl(1)-Ru(1)-Cl(2)	90.132(10)
C(22)-Ru(1)-Cl(1)	95.78(4)
C(1)-Ru(1)-Cl(2)	152.46(3)

Whilst Ru-O(1) bond length of **7a** is 2.154(2) Å, that of **7b** is shorter as 2.0981(8) Å. This difference of bond strength affected their reactivity of olefin metathesis (discussed below). Dependence of Ru-O bond length to ring size could be interpreted by steric of the ring compound. To evaluate chemical effects of steric strains, an effect termed I-strain was suggested for cyclic compounds. Specifically, I-strain refers to change in internal strain of a ring compound which arises from a change in the coordination number and the preferred bond angle of an atom of interest.[21] Both 5- and 7-membered rings are inherently strained to some extent due to the torsional forces about C-C single bonds. Geometrically more flexible caprolactam remains its most stable constellation when chelated compared to the reported crystallographic data of a bare caprolactam.[22] However, chelated pyrrolidinone cannot reduce the sterics around the amide bond as its 5-membered structure is less flexible than 7-membered caprolactam. It is indirectly supported by heats of combustion per methylene group for 5- and 7-membered cyclic alkanes. The reported values are 158.7 and 158.3 kcal/mol for cyclopentane and cycloheptane, respectively.[23] This indicates that 5-membered cyclic compound has slightly higher steric than 7-membered ring. (Simplified model as cyclic alkanes was used because direct comparison of 2-pyrrolidinone and caprolactam is not appropriate as they contain other types of bonds than methylene bonds.) While the angle around amide ketone functionality is close to 130° in complex **7a**, that of complex **7b** is approximately 121°. The more distorted bond prevents carbonyl of complex **7a** from reaching ruthenium center compared to complex **7b**. Hence, the Ru-O bond

length of **7a** becomes longer than that of **7b**. Another interpretation could arise from the enriched electron density of nitrogen. When vinyl lactam coordinates to ruthenium, i.e., after vinyl C-C double bond is replaced with Ru-C bond, nitrogen atom of lactam becomes electron richer. While nitrogen atom of 5-membered ring faces C-H bonds in pseudo-axial position, such steric effect is resolved by chair-like geometry of 7-membered compound. Such repulsion between nitrogen lone pair electron and C-H bond may also distort amide bond to affect ruthenium-carbonyl bond length.

In the NMR spectrum of complex **7a** in CD_2Cl_2, there were always two characteristic peaks at 13.5 and 12.5 ppm. While the major peak of 13.5 ppm was assigned as a carbenic proton, the identity of another was in question. To our surprise, strikingly different NMR spectrum was obtained when NMR spectra was recorded using C_6D_6 as a solvent. Firstly, the major peak was changed from 13.5 ppm to 12.5 ppm, which indicates they could be convertible in a solution phase. In addition, the other protons from NHC backbone and mesitylene group were all appeared as a singlet, unlike the spectrum taken in CD_2Cl_2, in which all protons were split (Figure 5).

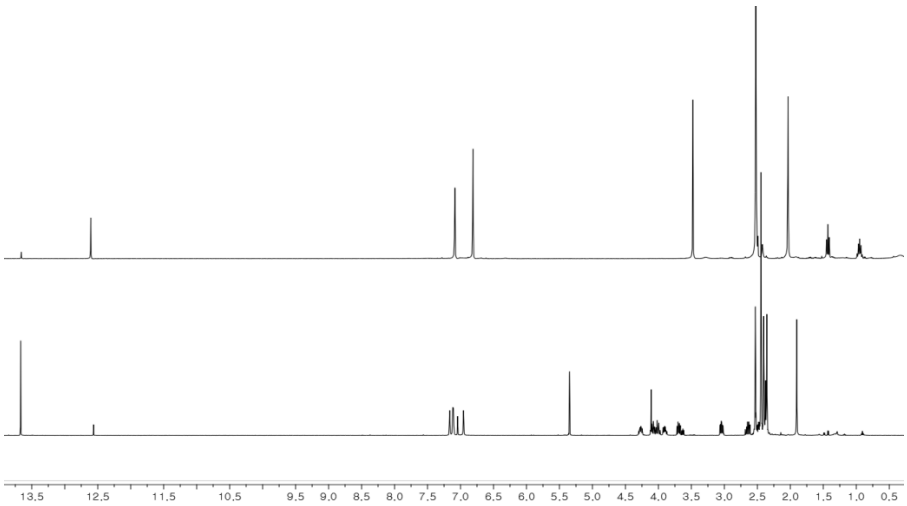

Figure 5. NMR spectrum of complex **7a** in CD_2Cl_2 at 25 °C (below) and C_6D_6 at 75 °C (above)

This phenomenon can be interpreted as a dynamic isomerization between *cis*-dichloro and *trans*-dichloro complexes. When the complex was dissolved in CD_2Cl_2, the isomers exist in 8:1 ratio and the protons for each isomer can be assigned in the spectrum. However, it converts to another isomer almost quantitatively in C_6D_6 at elevated temperature, and shows clear singlet patterns due to its symmetric character and free rotation of the NHC ligand. More interestingly, the unsymmetric nature of *cis*-dichloro isomer influenced the germinal lactam ring protons so that each proton appears separately in the spectrum.

When complex **7b** was dissolved in the same solvents, similar NMR pattern was observed (Table 4). It is postulated that polarity of solvent affects the isomerization since *trans*-dichloro complex has more

symmetric structure. Attempt to dissolve the complex in other solvents such as THF and dioxane was unsuccessful. Isomerization always occurred along with color change of the solution from brown to dark green. Once the majority species are converted from *cis*- to *trans*-dichloro isomer, the ratio didn't restore to the original state, which implicates this isomerization process is non-reversible.

Table 3. Ratio of *cis*- and *trans*-dichloro isomers of **7b**

Solvent	Relative Polarity	Temp. (°C)	Ratio (%*cis*:%*trans*)[a]
CD_2Cl_2	0.309	25	94:6
C_6D_6	0.111	40	59:41
		85	16:84

[a]Measured by NMR

Previously, similar isomerization of sulfur-chelated ruthenium olefin metathesis catalyst induced by UV-light was reported by A. Ben-Asuly et al.[16] In our case, it is believed to be the polarity of solvent influences the isomerization process. The mechanism of such isomerization was suggested to be relocation of the Ru-Cl bonds of 14 electron species followed by dissociation of chelating group.[24]

Reactivity Test. Ring-closing metathesis of diethyldiallyl malonate (DEDAM) was conducted to compare the reactivity of the complexes.

While Complex **7a** showed comparable RCM reactivity at ambient temperature, complex **7b** and had no reactivity at all as shown in Chart 1. This can be explained by the difference of initiation rate which is supported by the shorter Ru-O length of **7a** than that of **7b** as explained in previous section and revealed by their X-ray crystallographic data.

Chart 1. RCM of DEDAM at 25 °C in CD_2Cl_2

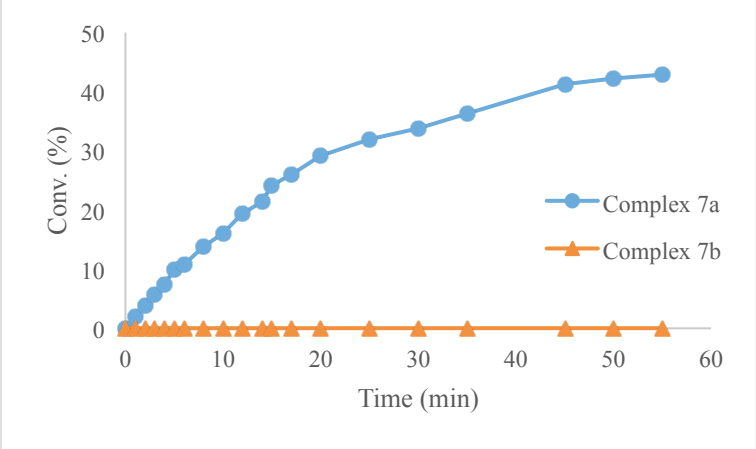

When the reaction temperature was increased to achieve higher conversion, however, unexpected result was achieved. While complex **7a** afforded ring-closed product in >99% conversion within half an hour, complex **7b** catalyzed the reaction very slowly (Chart 2). Moreover, as revealed by its NMR spectra, complex **7b** afforded ring closing metathesis only in minor yield. Rather, it promoted cycloisomerization reaction which is known to be catalyzed by ruthenium hydride species.[25] It is supported by the appearance of the hydride peak in NMR spectra and distinct color change to orange-

yellow which is a representative character of ruthenium hydride species. It was reported that ruthenium-carbene species designed for olefin metathesis could catalyze such reactions in a non-metathetic way.[26,27]

Chart 2. RCM of DEDAM at 85 °C in CD_5CD_3

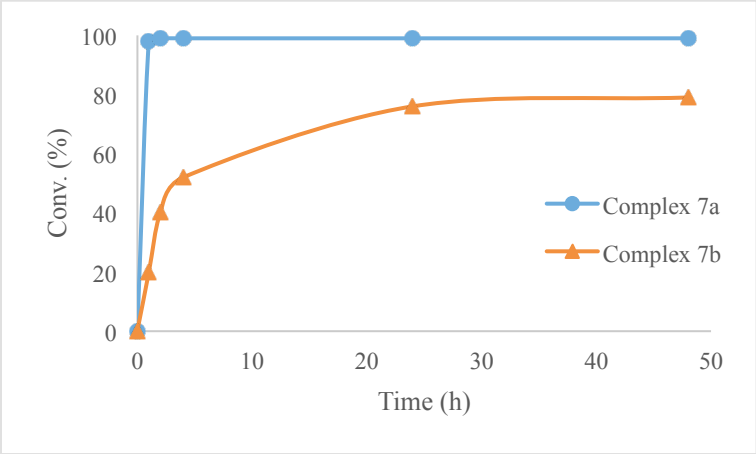

To further study the reaction of complex **7b**, various solvents were tested. The selection of solvent depended on its polarity because the catalyst showed structural difference when the solvent varied. The ratio of RCM and cycloisomerization products highly depends on solvents (Table 1). Polar solvent such as dichloromethane didn't afford any product for both reaction, but less polar benzene gave cycloisomerization product in 84% yield along with 4.8 of RCM yield (Entry 4). When the polar solvent with higher boiling point, for example, dichloroethane or tetrachloroethane was used to increase the reaction temperature, ring-closing metathesis was dominant but the yield was poor (Entry 7, 27%).

Table 4. RCM versus cycloisomerization depending on the solvent

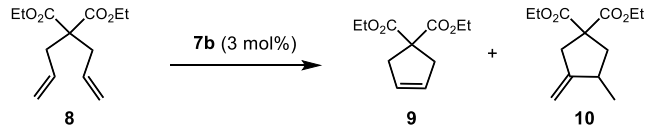

8 9 10

Entry	Solvent	Temp. (°C)	Time (h)	Yield of 9 (%)[a]	Yield of 10 (%)[a]
1	CD_2Cl_2	25	1	0	0
2	CD_2Cl_2	40	24	0	0
3	C_6D_6	85	1	<1	29
4	C_6D_6	85	48	4.8	84
5	$C_2D_4Cl_2$	75	22	3.6	36
6	$C_2D_2Cl_4$	75	7	0	0
7	$C_2D_2Cl_4$	120	24	27	7

[a]Measured by NMR;

Conclusion

In an attempt to develop a novel ruthenium olefin metathesis catalyst, two complexes with chelating *N*-vinyl lactam were synthesized. It was expected that the combination of electron donating effect of nitrogen atom adjacent to the carbenic carbon and labile carbonyl chelation would afford highly reactive metathesis catalysts with its stability remained. However, the complexes didn't show greater olefin metathesis reactivity compared to the commercially available ruthenium olefin metathesis catalysts. 5-membered lactam ligand afforded comparably reactive catalyst. 7-membered lactam-coordinated complex was unreactive toward olefin metathesis, however, upon thermal stimuli it catalyzed cycloisomerization reaction in a high yield. Another interesting feature of the complexes was that it showed *cis*- and *trans*-dichloro isomerization behavior depending on the polarity of the solvent.

This study showed that *N*-vinyl lactam can be used as a ligand for olefin metathesis catalysts. Combination of chelating property of carbonyl group and electron-richness of ruthenium center induced by Fischer carbene can pave a new way in olefin metathesis catalyst development. It is expected that further study by varying electronic property of the chelating ligand would result highly effective catalysts.

Experimental Section

Compound **7a**: *N*-vinyl caprolactam (0.24 mmol) and second generation Grubbs catalyst (0.12 mmol) were dissolved in dichloromethane (5 mL) in a 10 mL schlenk tube. The reaction mixture was stirred at room temperature for 5 h. The resulting mixture was filtered through celite, then concentrated to 2-3 mL dichloromethane. After the reaction, CH_2Cl_2 was reduced to minimal amount and recrystallization in diethylether followed by washing with pentane gave the product (60%). Crystals suitable for X-ray were obtained by slow diffusion between pentane and a solution of **2** in dichloromethane. ^{1}H NMR (CD_2Cl_2, 400 MHz) : δ 13.41 (s, 1H), 7.11-6.88 (m, 4H), 4.20-4.16 (m, 1H), 3.97-3.78 (m, 3H), 3.47-3.39 (m, 2H), 2.97-2.92 (m, 1H), 2.60-2.30 (m, 16H), 1.88-1.72 (m, 6H), 1.50-1.30 (m, 3H) ^{13}C NMR (CD_2Cl_2, 100 MHz) : 217.1, 185.2, 139.9, 139.8, 138.9, 138.6, 137.8, 135.5, 131.8, 131.5, 130.1, 129.8, 129.3, 128.7, 55.5, 53.9, 51.0, 34.5, 29.6, 27.9, 23.2, 21.0, 19.6, 18.0, 17.9, 16.9.

Compound **7b**: 1-vinyl-2-pyrrolidinone (0.24 mmol), cuprous chloride (0.12 mmol) and second generation Grubbs catalyst (0.12 mmol) were dissolved in dichloromethane (5 mL) in a 10 mL schlenk tube. The reaction mixture was stirred at room temperature for 3 h. (The consumption of second generation Grubbs catalyst was monitored by ^{1}H NMR). The resulting mixture was filtered through celite, then

concentrated to 2-3mL dichloromethane. Crude product was purified by recrystallization in diethylether followed by washing with pentane to afford the desired product. Recrystallization from a mixture pentane and dichloromethane afforded **7b**, as maroon crystals in 40 % yield. ^{1}H NMR (CD_2Cl_2, 400 MHz) :δ 13.50 (s, 1H), 6.98 (s, 2H), 6.88 (s, 2H), 3.96 (m, 4H), 2.43-2.44 (ss, 18H), 2.12-2.03 (m, 2H), 3.51 (m, 1H), 2.92 (m, 1H), 1.77-1.64 (m, 2H) ^{13}C NMR (CD_2Cl_2, 100 MHz) : 216.7, 185.9, 139.2, 138.8, 138.6, 138.4, 138.0, 136.4, 136.3, 131.1, 130.0, 129.4, 128.8, 125.2, 124.9, 123.8, 51.1, 46.9, 31.0, 27.6, 27.2, 26.0, 22.9, 20.9, 17.9.

General procedure for RCM reactions. Typically 5 mol % of the catalyst was added to a solution of substrate (0.10 mmol) using capped NMR tube in 0.5 ml of deuterated solvent. When necessary, the reaction was heated in the NMR probe and analyzed by arrayed experiment.

Reference

(1) *Handbook of Metathesis*; Grubbs, R. H. ed.; Wiley-VCH: Weinhein, Germany, 2003.

(2) *Olefin Metathesis: Theory and Practice*; Grela, Karol ed.; John Wiley & Sons: Hoboken, New Jersey, 2014.

(3) Hoveyda, A. H.; Zhugralin, A. R. *Nature* **2007**, *450*, 243.

(4) Trnka, T. M.; Grubbs, R. H. *Acc. Chem. Res.* **2000**, *34*, 18.

(5) Schrock, R. R.; Hoveyda, A. H. *Angew. Chem. Int. Ed.* **2003**, *42*, 4592.

(6) Vougioukalakis, G. C.; Grubbs, R. H. *Chem. Rev.* **2010**, *110*, 1746.

(7) Scholl, M.; Ding, S.; Lee, C. W.; Grubbs, R. H. *Organic Letters* **1999**, *1*, 953.

(8) Garber, S. B.; Kingsbury, J. S.; Gray, B. L.; Hoveyda, A. H. *J. Am. Chem. Soc.* **2000**, *122*, 8168.

(9) Michrowska, A.; Bujok, R.; Harutyunyan, S.; Sashuk, V.; Dolgonos, G.; Grela, K. *J. Am. Chem. Soc.* **2004**, *126*, 9318.

(10) Tzur, E.; Szadkowska, A.; Ben-Asuly , A.; Makal, A.; Goldberg, I.; Woźniak, K.; Grela , K.; Lemcoff, N. G. *Chemistry – A European Journal* **2010**, *16*, 8726.

(11) Slugovc, C.; Perner, B.; Stelzer, F.; Mereiter, K. *Organometallics* **2004**, *23*, 3622.

(12) Slugovc, C.; Burtscher, D.; Stelzer, F.; Mereiter, K. *Organometallics* **2005**, *24*, 2255.

(13) Fürstner, A.; Thiel, O. R.; Lehmann, C. W. *Organometallics* **2001**, *21*, 331.

(14) Hejl, A.; Day, M. W.; Grubbs, R. H. *Organometallics* **2006**, *25*, 6149.

(15) Hansen, S. M.; Volland, M. A. O.; Rominger, F.; Eisenträger, F.; Hofmann, P. *Angew. Chem. Int. Ed.* **1999**, *38*, 1273.

(16) Ben-Asuly, A.; Aharoni, A.; Diesendruck, C. E.; Vidavsky, Y.; Goldberg, I.; Straub, B. F.; Lemcoff, N. G. *Organometallics* **2009**, *28*, 4652.

(17) Louie, J.; Grubbs, R. H. *Organometallics* **2002**, *21*, 2153.

(18) Wu, Z.; Nguyen, S. T.; Grubbs, R. H.; Ziller, J. W. *J. Am. Chem. Soc.* **1995**, *117*, 5503.

(19) Thomas, R. M.; Fedorov, A.; Keitz, B. K.; Grubbs, R. H. *Organometallics* **2011**, *30*, 6713.
(20) Dixneuf, P. H.; Romero, A.; Vegas, A. *Angew. Chem., Int. Ed.* **1990**, *29*, 215.
(21) Brown, H. C.; Gerstein, M. *J. Am. Chem. Soc.* **1950**, *72*, 2926.
(22) Oya, K. P.; Myasnikova, R. M. *J. Struct. Chem.* **1974**, *15*, 578.
(23) Spitzer, R.; Huffman, H. M. *J. Am. Chem. Soc.* **1947**, *69*, 211.
(24) Barbasiewicz, M.; Szadkowska, A.; Bujok, R.; Grela, K. *Organometallics* **2006**, *25*, 3599.
(25) Yamamoto, Y.; Nakagai, Y.-i.; Ohkoshi, N.; Itoh, K. *J. Am. Chem. Soc.* **2001**, *123*, 6372.
(26) Schmidt, B. *Eur. J. Org. Chem.* **2004**, *2004*, 1865.
(27) Terada, Y.; Arisawa, M.; Nishida, A. *Angew. Chem. Int. Ed.* **2004**, *43*, 4063.

Supplementary Information

Table of Contents

1. Method and Materials

All reactions were carried out using standard Schlenk techniques, or in an argon-filled glove box unless otherwise mentioned. Deuterated solvents were dried under the calcium hydride and vacuum transferred prior to use. NMR spectra were obtained on an Agilent 400-MR DD2 Magnetic Resonance System (400 MHz). Chemical shift values were recorded in ppm relative to tetramethylsilane (TMS) as an internal standard, and coupling constants in Hertz (Hz). Grubbs catalyst second generation was purchased from Sigma-Aldrich. Most substrates were obtained from commercial suppliers and used as received without further purification.

2. Spectra

Complex 7a

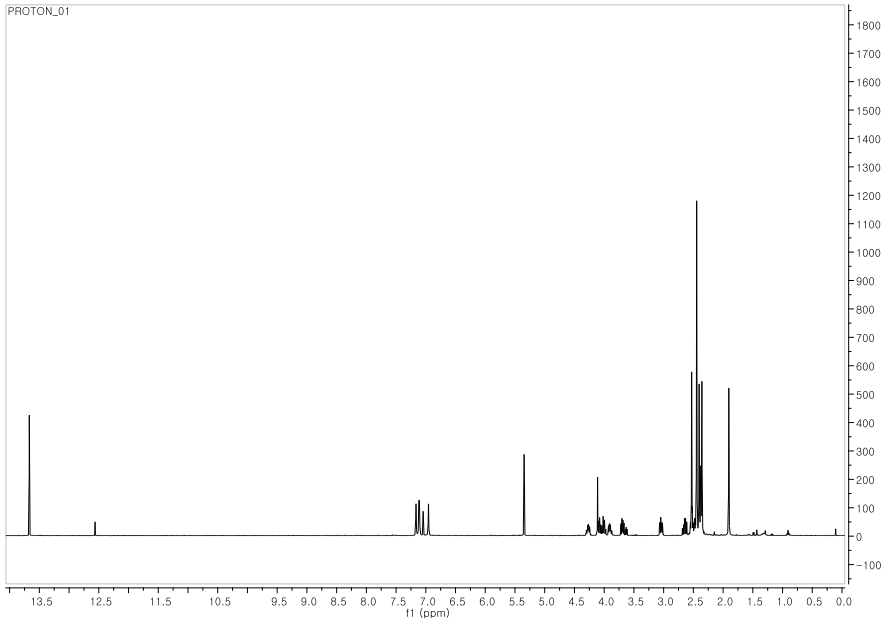

^{1}H NMR (500 MHz, CD_2Cl2) mixture of *cis*-dichloro and *trans*-dichloro complexes (ratio 8:1)
***cis*-dichloro** δ 13.65 (s, 1H), 7.14 (s, 1H), 7.09 (d, *J* = 5.1 Hz, 2H), 6.95 (d, *J* = 14.8 Hz, 1H), 4.35 – 4.21 (m, 1H), 4.10 – 3.95 (m, 2H), 3.89 (dd, *J* = 10.6,

5.9 Hz, 1H), 3.69 – 3.64 (m, 1H), 3.04 – 2.99 (dt, 1H), 2.66 – 2.58 (m, 1H), 2.50 (s, 3H), 2.42 (s, 6H), 2.38 (s, 3H), 2.33 (s, 3H), 1.88 (s, 3H)

***trans*-dichloro** δ 12.54 (s, 1H), 7.02 (s, 4H), 4.09 (s, 4H), 3.61 (t, 2H), 2.50 – 2.43 (m, 2H), 2.42 (s, 6H), 2.35 (s, 12H)

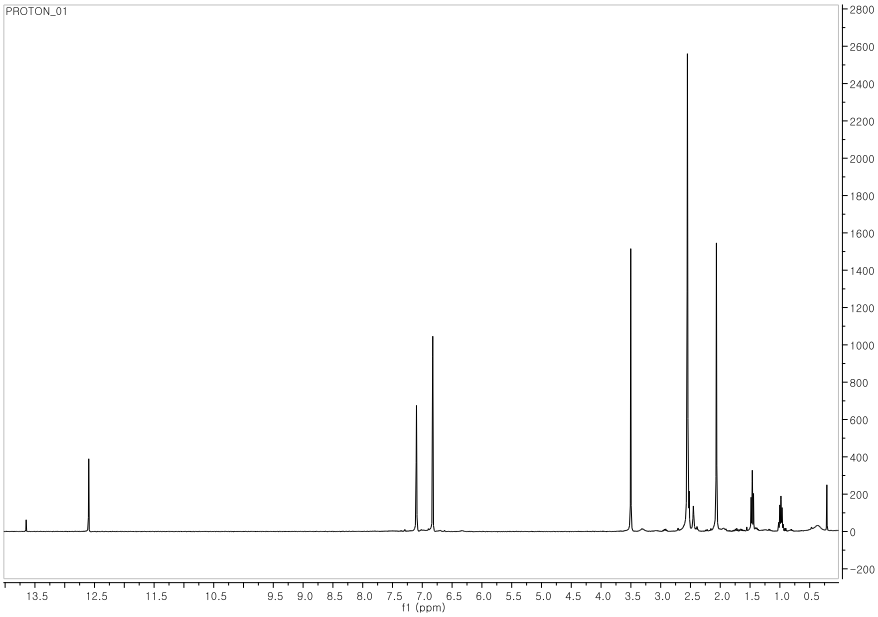

^{1}H NMR (400 MHz, C_6D_6, 75 °C) δ 12.66 (s, 4H), 6.89 (s, 4H), 3.57 (s, 4H), 2.60 (s, 12H), 2.13 (s, 6H), 1.59 – 1.45 (m, 2H), 1.14 – 0.98 (m, 2H).

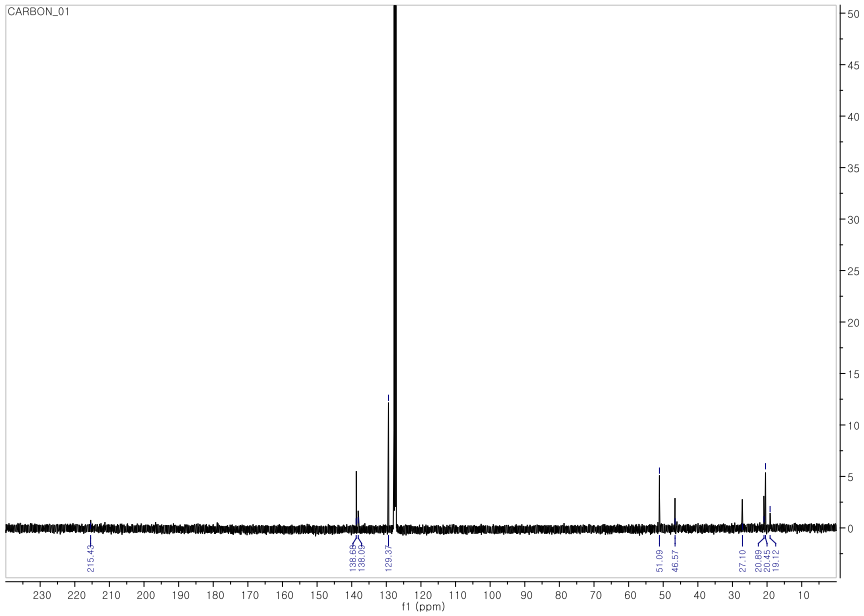

^{13}C NMR (100 MHz, C_6D_6) δ 215.43, 138.68, 138.09, 129.37, 51.09, 46.57, 27.15, 20.89, 20.45, 19.12.

Complex 7b

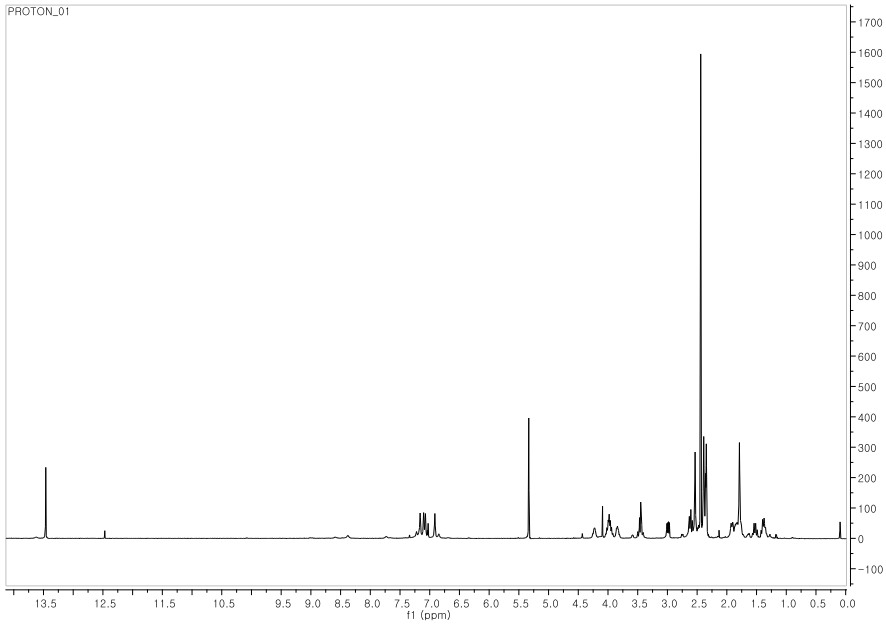

^{1}H NMR (500 MHz, CD_2Cl2) *cis*-dichloro as large majority
δ 13.46 (s, 1H), 7.27 – 7.03 (m, 3H), 6.88 (d, *J* = 33.3 Hz, 1H), 4.27 – 4.11 (m, 1H), 4.07 – 3.80 (m, 2H), 3.78-3.75 (m, 1H), 3.44 (dd, *J* = 22.6, 7.9 Hz, 1H), 2.99 (dd, *J* = 14.0, 7.1 Hz, 1H), 2.72 – 1.31 (m, 26H)

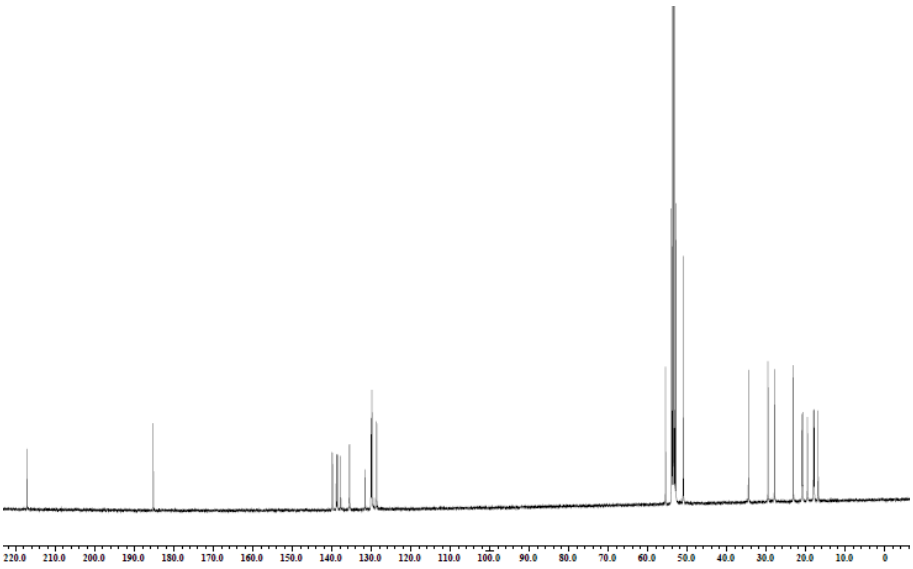

^{13}C NMR (100 MHz, CD_2Cl_2) 216.7, 185.9, 139.2, 138.8, 138.6, 138.4, 138.0, 136.4, 136.3, 131.1, 130.0, 129.4, 128.8, 125.2, 124.9, 123.8, 51.1, 46.9, 31.0, 27.6, 27.2, 26.0, 22.9, 20.9, 17.9.

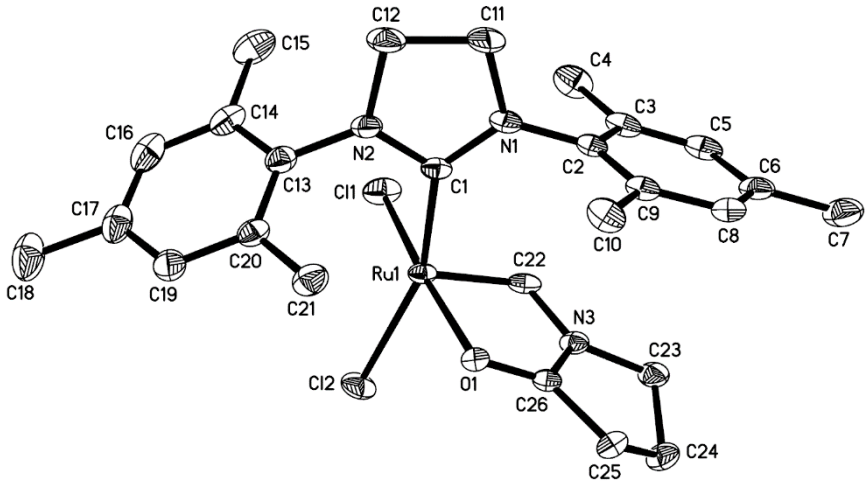

F**igure S1.** Molecular structure of complex **7a**.

Table S1. Crystal data and structure refinement for complex **7a**.

Identification code	hsh61	
Empirical formula	C27 H35 Cl4 N3 O Ru	
Formula weight	660.45	
Temperature	103(2) K	
Wavelength	0.71073 Å	
Crystal system	Triclinic	
Space group	P-1	
Unit cell dimensions	a = 11.8364(4) Å	α= 71.9080(10)°.
	b = 15.0197(5) Å	β= 89.1890(10)°.
	c = 17.3630(5) Å	γ = 77.9660(10)°.
Volume	2865.43(16) $Å^3$	
Z	4	
Density (calculated)	1.531 Mg/m^3	
Absorption coefficient	0.946 mm^{-1}	
F(000)	1352	
Crystal size	0.40 x 0.40 x 0.38 mm^3	
Theta range for data collection	1.24 to 31.08°.	

Index ranges	-17<=h<=17, -21<=k<=21, -25<=l<=19
Reflections collected	80314
Independent reflections	18200 [R(int) = 0.0398]
Completeness to theta = 31.08°	98.9 %
Absorption correction	Semi-empirical from equivalents
Max. and min. transmission	0.7151 and 0.7035
Refinement method	Full-matrix least-squares on F^2
Data / restraints / parameters	18200 / 106 / 689
Goodness-of-fit on F^2	1.073
Final R indices [I>2sigma(I)]	R1 = 0.0478, wR2 = 0.1264
R indices (all data)	R1 = 0.0646, wR2 = 0.1459
Largest diff. peak and hole	2.527 and -2.322 e.$Å^{-3}$

Table S1. Selected bond lengths (Å) and angles (°) for complex **7a**.

Ru(1)-C(22)	1.816(3)	C(22)-Ru(1)-C(1)	99.44(13)
Ru(1)-C(1)	1.993(3)	C(22)-Ru(1)-O(1)	79.80(11)
Ru(1)-O(1)	2.154(2)	C(1)-Ru(1)-O(1)	95.66(10)
Ru(1)-Cl(1)	2.3446(8)	C(22)-Ru(1)-Cl(1)	94.29(10)
Ru(1)-Cl(2)	2.3786(8)	C(22)-Ru(1)-Cl(2)	101.91(9)
C(22)-N(3)	1.382(4)	C(1)-Ru(1)-Cl(2)	158.64(9)
C(22)-H(22)	0.9500	O(1)-Ru(1)-Cl(2)	87.44(6)
C(19)-H(19)	1.513(5)	Cl(1)-Ru(1)-Cl(2)	92.42(3)
C(23)-N(3)	1.476(4)	N(3)-C(22)-Ru(1)	116.4(2)
C(23)-C(24)	1.538(5)	N(3)-C(22)-H(22)	121.8
C(23)-H (23A)	0.9900	N(3)-C(23)-C(24)	101.6(3)
C(23)-H(23B)	0.9900	C(25)-C(24)-C(23)	105.1(3)
C(24)-C(25)	1.532(4)	C(26)-C(25)-C(24)	101.8(3)
C(24)-H(24A)	0.9900	O(1)-C(26)-N(3)	119.3(3)
C(24)-H(24B)	0.9900	O(1)-C(26)-C(25)	130.4(3)
C(25)-C(26)	1.494(4)	N(3)-C(26)-C(25)	110.3(3)
C(25)-H(25A)	0.9900	C(26)-N(3)-C(22)	115.3(3)
C(25)-H(25B)	0.9900	C(22)-N(3)-C(23)	132.0(3)
C(26)-O(1)	1.252(4)		
C(26)-N(3)	1.350(4)		

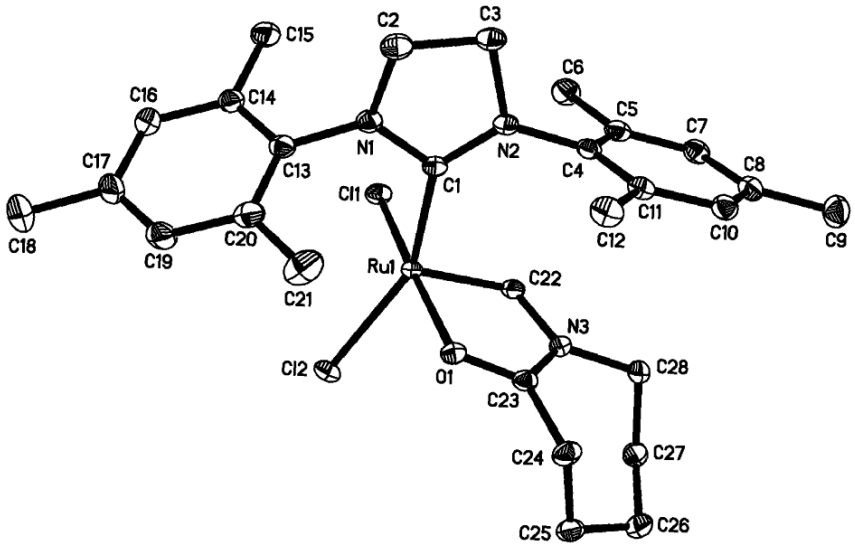

Figure S2. Molecular structure of complex **7b**.

Table S3. Crystal data and structure refinement for complex **7b**.

Identification code	hsh54s	
Empirical formula	C29 H39 Cl4 N3 O Ru	
Formula weight	688.50	
Temperature	103(2) K	
Wavelength	0.71073 Å	
Crystal system	Monoclinic	
Space group	P2(1)/c	
Unit cell dimensions	a = 11.6929(3) Å	α= 90°.
	b = 12.7939(3) Å	β= 104.8350(10)°.
	c = 21.9609(5) Å	γ = 90°.
Volume	3175.79(13) $Å^3$	
Z	4	
Density (calculated)	1.440 Mg/m^3	
Absorption coefficient	0.857 mm^{-1}	
F(000)	1416	
Crystal size	0.40 x 0.40 x 0.14 mm^3	

Theta range for data collection	2.49 to 34.12°.
Index ranges	-17<=h<=18, -20<=k<=19, -34<=l<=33
Reflections collected	53589
Independent reflections	13041 [R(int) = 0.0298]
Completeness to theta = 34.12°	99.6 %
Absorption correction	Semi-empirical from equivalents
Max. and min. transmission	0.8895 and 0.7257
Refinement method	Full-matrix least-squares on F^2
Data / restraints / parameters	13041 / 0 / 349
Goodness-of-fit on F^2	1.033
Final R indices [I>2sigma(I)]	R1 = 0.0247, wR2 = 0.0599
R indices (all data)	R1 = 0.0311, wR2 = 0.0631
Largest diff. peak and hole	0.975 and -0.865 e.$Å^{-3}$

Table S4. Selected bond lengths (Å) and angles (°) for complex **7b**.

Ru(1)-C(22)	1.8159(11)	C(22)-Ru(1)-C(1)	97.61(5)
Ru(1)-C(1)	1.9929(11)	C(22)-Ru(1)-O(1)	78.75(4)
Ru(1)-O(1)	2.0981(8)	C(1)-Ru(1)-O(1)	95.51(4)
Ru(1)-Cl(1)	2.3510(3)	C(22)-Ru(1)-Cl(1)	95.78(4)
Ru(1)-Cl(2)	2.3729(3)	C(1)-Ru(1)-Cl(1)	89.21(3)
C(22)-N(3)	1.3924(14)	O(1)-Ru(1)-Cl(1)	173.18(2)
C(22)-H(22)	0.9500	C(22)-Ru(1)-Cl(2)	109.84(3)
C(23)-O(1)	1.2540(14)	C(1)-Ru(1)-Cl(2)	152.46(3)
C(23)-N(3)	1.3555(15)	O(1)-Ru(1)-Cl(2)	87.95(2)
C(23)-C(24)	1.4908(16)	Cl(1)-Ru(1)-Cl(2)	90.132(10)
C(24)-C(25)	1.5402(17)	N(3)-C(22)-Ru(1)	118.18(8)
C(24)-H(24A)	0.9900	N(3)-C(22)-H(22)	120.90
C(24)-H(24B)	0.9900	Ru(1)-C(22)-H(22)	120.90
C(25)-C(26)	1.527(2)	O(1)-C(23)-N(3)	117.26(10)
C(25)-H(25A)	0.9900	O(1)-C(23)-C(24)	121.53(11)
C(25)-H(25B)	0.9900	N(3)-C(23)-C(24)	121.13(10)
C(26)-C(27)	1.527(2)	C(23)-C(24)-C(25)	111.19(9)
C(26)-H(26A)	0.9900	C(26)-C(25)-C(24)	114.64(10)
C(26)-H(26B)	0.9900	C(25)-C(26)-C(27)	116.22(10)
C(27)-C(28)	1.5234(17)	C(28)-C(27)-C(26)	114.49(11)
C(27)-H(27A)	0.9900	N(3)-C(28)-C(27)	112.55(10)
C(27)-H(27B)	0.9900		
C(28)-N(3)	1.4754(15)		
C(28)-H(28A)	0.9900		
C(28)-H(28B)	0.9900		

요약문

올레핀 메타테시스 반응은 탄소간의 이중 결합을 재배치하여 새로운 이중 결합 분자를 형성하는 반응이다. 이 반응에는 루테늄, 텅스텐, 몰리브데늄 등의 금속 촉매가 널리 알려져 있으며, 특히 루테늄 촉매는 공기 또는 수분과의 접촉에 다른 금속보다 덜 민감하므로 유기화학 분야에서 널리 사용되고 있다. 본 연구에서는 *N*-비닐 락탐을 리간드로 사용하여 전자밀도가 풍부한 금속 중심 원자를 지님과 동시에 락탐의 키톤기가 금속 중심 원자에 배위하여 빠른 초기 속도를 가지도록 촉매 구조를 고안하였다. 다른 고리 크기를 가진 두 종류의 락탐을 이용하여 촉매를 합성하였을 때, 기대한 바와 같이 메타테시스 반응성이 관찰되긴 하였으나 상용화된 촉매들보다 우수하지 않은 수율을 나타내었다. 반응성을 증대시키기 위해 고온에서 반응을 진행하면 메타테시스 수율은 낮아지고 고리이성질화 반응을 촉매하였으며, 반응의 최대 수율은 84%이다. 또한 본 연구에서 합성된 촉매는 용매의 극성에 따라 용액 상에서 시스-디클로로 또는 트랜스-디클로로 구조를 갖는다. 이러한 구조 변화는 기존 연구에서 종종 보고되었으나, 용매에 의존하여 이성질화가 이루어지는 것은 드물게 관찰되지 않았던 특징이다.

본 연구를 통해 *N*-비닐 락탐이 올레핀 메타테시스 촉매의 리간드로 사용될 수 있음을 보였다. 키톤기의 배위, 피셔 카빈에서 기인하는 전자가 풍부한 루테늄 등의 특징이 새로운 형태의 메타테시스 촉매 개발을 가능하게 하였다. 리간드로 사용되는 아마이드의 전자적 성질을 변화시키는 차후 연구를 통해 이러한 촉매의 반응성의 증대가 기대된다.